Story Operators: A Reproducing Kernel Hilbert Space Framework for Narrative Discovery and Transformation

Fred Zimmerman
Story Operators New Media / Nimble Books LLC, Ann Arbor, MI
wfz@nimblebooks.com

April 2026

Abstract

I develop a unified mathematical framework—"Story Operators"—for narrative analysis and transformation built on Reproducing Kernel Hilbert Space (RKHS) theory. Texts are mapped into a 768- or 1024-dimensional embedding space via sentence-transformer feature maps; similarity is measured by an explicit family of fifteen positive semi-definite narrative kernels (cosine, RBF, Global Alignment, scene co-occurrence, theme activation, escalation graph, and composites); and content is transformed by thirty-four bounded linear operators defined intrinsically on the RKHS. I prove that all proposed kernels are PSD via the standard closure properties (sum, product, composition, exponentiation, normalization) and that the resulting operators are non-expansive on the unit sphere. Empirically, I instantiate the framework on *CodexSpace*, a 28,602-book embedded universe derived from the PG-19 corpus, and on extensions to Books3 (52,796 modern books) and the IB1 Internet Archive corpus (452,796 books). I report (i) a 25-cluster structure recovering ten major literary genres covering 88.3% of the corpus, (ii) a doctrine-morphing experiment in which ten operators applied to 105 strategic doctrines yield 16 validated novel concepts (1.5% yield, novelty scores 0.745–0.822), (iii) RKHS-First publishing pilots in which designed-then-written books improve convex-hull coverage by 60% and minimum chapter distance by 89% relative to traditionally-structured matched controls, and (iv) corpus-scale novelty trajectories (the running-centroid measure) showing modern books are roughly 10% more novel than pre-1920 books and modernist free verse is $\sim 7\times$ more circuitous than formal verse. All embedding files, kernels, and operators are deployed as a public toolkit at https://bigfivekiller.online. The framework is intended both as a foundation for computational narratology and as production infrastructure for AGI-era publishing.

Keywords: RKHS, kernel methods, computational narratology, sentence embeddings, narrative operators, optimal transport, semantic novelty, distant reading, publishing economics.

1 Introduction

Computational analysis of narrative has historically split into two loosely connected lines of work: lexical and topic-based "distant reading" (Moretti 2005; Jockers 2013; Underwood 2019), which treats texts as bags of words or topic mixtures; and sentiment-arc modelling (Reagan et al. 2016; Vonnegut 1981), which reduces a story to a one-dimensional emotional trajectory. Both have produced striking results, but neither offers a structured *algebra* on stories. There is no widely accepted way to write down "T applied to *Romeo and Juliet* yields *West Side Story*" as a mathematical statement, much less to compose, invert, or compare such operators across thousands of books.

This paper, distilled from a longer monograph (F. Zimmerman 2026e), argues that the missing ingredient is the right *ambient space*. Once a corpus is embedded into a Reproducing Kernel Hilbert Space (RKHS), the ordinary toolkit of functional analysis—inner products, projections, geodesics, spectral decompositions, optimal transport, bounded linear operators—becomes directly available. An RKHS is exactly the structure in which *similarity*, *geometry*, and *transformation* are mutually compatible: the kernel determines the inner product, the inner product determines the geometry, and the geometry constrains the operators.

What is new. Most previous applications of kernel methods to text have been discriminative (text classification, sentence-pair scoring, retrieval). What I add is:

1. A *family* of fifteen positive semi-definite (PSD) narrative kernels, each constructed from explicit feature maps or closure operations, covering character networks (Labatut and Bost 2019), narrative arcs (Cuturi 2011; Reagan et al. 2016), themes, tensions, escalation graphs (Shervashidze et al. 2011), and prosody (Section 3).
2. A catalogue of thirty-four bounded linear operators defined intrinsically on the RKHS, organised by domain—ten doctrine operators, fourteen fiction operators, ten poetry operators (Sections 4 and Appendix B).
3. A public empirical apparatus—*CodexSpace* on PG-19 (Rae et al. 2020) and its extensions to Books3 (Gao et al. 2021) and the Internet Archive's IB1 corpus—providing reproducible quantitative findings at three scales: 2.86×10^4, 8.15×10^4, and 4.53×10^5 books.
4. A set of cross-domain applications—doctrine morphing (F. Zimmerman 2026b), story liberation, RKHS-first publishing, novelty-curve diagnostics (F. Zimmerman 2026d; F. Zimmerman 2026c; W. F. Zimmerman 2026)—each accompanied by quantitative metrics and limitations.

Stance. I do not claim that RKHS exhausts the structure of narrative; the manifold hypothesis (Section 8) limits the truly admissible region of $\mathcal{H}_N$ to a low-dimensional submanifold, and psychological similarity violates symmetry in ways no PSD kernel can mimic (Tversky 1977). But I do claim that RKHS is the *minimal* mathematical setting in which the operations practitioners already perform informally—"find books like this," "shift this story to a new genre," "identify a gap in the catalog"—become well-defined, composable, and reproducible.

Why now. Three independent developments converged to make the framework viable in 2025–2026. First, sentence-transformer embeddings (Reimers and Gurevych 2019; Muennighoff et al. 2023) reached the quality threshold at which kernel-based downstream analysis is meaningful; prior to roughly 2019, sentence embeddings were too noisy. Second, single-machine compute (laptop CPUs and entry-level GPUs) became sufficient to embed and store hundreds of thousands of books without distributed infrastructure—the IB1 corpus (W. F. Zimmerman 2026) of 452,796 books fits in ~ 20 GB of `float16` storage on a single SSD. Third, large language models reached the quality threshold at which the inverse embedding problem (Section 6.5) is tractable for production pipelines, making operator outputs realisable as fluent text in minutes rather than months. The mathematical apparatus existed for decades (Aronszajn 1950); the engineering only recently caught up.

Historical context. Three precedents anchor the methodological argument (F. Zimmerman 2026e, Ch. 1). Genetics before Shannon (1948)'s contemporary R. A. Fisher was largely descriptive; statistical genetics turned it into a predictive science. Chemistry before Mendeleev consisted of

a catalogue of known elements; the periodic table organised the catalogue and predicted gallium, germanium, and scandium before they were discovered. Linguistics before Chomsky was primarily taxonomic; formal grammar revealed deep cross-linguistic commonalities. In each case, mathematics did not replace domain expertise but multiplied its power. Story Operators stands in this lineage: not a replacement for editorial judgement, but a structured environment that makes it scalable, reproducible, and computable.

Roadmap. Section 2 establishes RKHS preliminaries. Section 3 introduces the narrative kernel family. Section 4 formalises Story Operators. Section 5 describes the empirical apparatus (CodexSpace and the deployed toolkit). Section 6 reports findings. Section 7 surveys applications, including doctrine morphing and RKHS-first publishing. Section 8 treats the narrative manifold, optimal transport, and spectral decomposition. Section 9 situates the work in the literature and weaves in related Zimmerman preprints. Section 12 discusses limitations. Appendices A–C give formal definitions, the operator catalogue, and reproducibility information.

2 Mathematical Preliminaries

I collect the RKHS facts needed below. Standard references are Aronszajn (1950), Berlinet and Thomas-Agnan (2004), Schölkopf and Smola (2002), and Steinwart and Christmann (2008).

Definition 2.1 (Reproducing kernel Hilbert space)**.** Let $\mathcal{X}$ be a non-empty set. A Hilbert space $\mathcal{H}$ of real-valued functions $f : \mathcal{X} \to \mathbb{R}$ is a *reproducing kernel Hilbert space* (RKHS) with kernel $k : \mathcal{X} \times \mathcal{X} \to \mathbb{R}$ if (i) $k(\cdot, x) \in \mathcal{H}$ for every $x \in \mathcal{X}$ and (ii) the reproducing property holds:

$$f(x) = \langle f,\, k(\cdot, x)\rangle_{\mathcal{H}}\,, \qquad \forall f \in \mathcal{H},\, x \in \mathcal{X}.$$

Definition 2.2 (Positive semi-definite kernel)**.** $k : \mathcal{X} \times \mathcal{X} \to \mathbb{R}$ is positive semi-definite (PSD) if for any finite $\{x_1, \ldots, x_n\} \subset \mathcal{X}$ the Gram matrix $\mathbf{K}_{ij} = k(x_i, x_j)$ is symmetric and positive semi-definite.

Theorem 2.1 (Moore–Aronszajn)**.** *Every PSD kernel k uniquely determines an RKHS $\mathcal{H}_k$ in which k is the reproducing kernel. Conversely, every RKHS has a unique PSD reproducing kernel.*

Proposition 2.2 (Closure properties)**.** *Let k_1, k_2 be PSD kernels on $\mathcal{X}$. Then the following constructions are PSD:*

1. *Non-negative combination: $ak_1 + bk_2$ for $a, b \geq 0$.*
2. *Pointwise product: $k_1 \cdot k_2$.*
3. *Composition with feature map: $k(\varphi(x), \varphi(y))$ for any $\varphi : \mathcal{X}' \to \mathcal{X}$.*
4. *Exponentiation: $\exp(k)$.*
5. *Normalization: $\widetilde{k}(x, y) = k(x, y)/\sqrt{k(x, x)\, k(y, y)}$ when $k(x, x) > 0$.*

I denote the embedding feature map of any PSD kernel k by $\varphi_k : \mathcal{X} \to \mathcal{H}_k$ with $k(x, y) = \langle \varphi_k(x),\, \varphi_k(y)\rangle_{\mathcal{H}_k}$.

Remark 2.1 (Embedding model). Throughout this paper a "narrative" N is encoded as a finite piece of text (a passage, chapter, or whole book), and the *base feature map* is the sentence-transformer

encoder $\varphi : \mathcal{X} \to \mathbb{R}^{768}$ given by all-mpnet-base-v2 (Reimers and Gurevych 2019), projected to the unit sphere S^{767}. The base kernel is therefore the cosine kernel

$$k_{\cos}(N_1, N_2) \;=\; \frac{\langle \varphi(N_1),\, \varphi(N_2) \rangle}{\|\varphi(N_1)\|\, \|\varphi(N_2)\|} \;=\; \langle \widehat{\varphi}(N_1),\, \widehat{\varphi}(N_2) \rangle\,.$$

A 1024-dimensional variant uses BGE-large-en-v1.5 for finer cluster resolution; the framework is otherwise unchanged.

Remark 2.2 (The kernel trick, in this setting). The classical motivation for kernel methods is the so-called *kernel trick*: an algorithm that depends on inputs only through inner products can be applied in $\mathcal{H}_N$ without ever computing φ explicitly (Schölkopf and Smola 2002). In the present setting φ *is* computed (it is the transformer forward pass), but the kernel-trick perspective remains valuable: every operation in subsequent sections, from genre transforms to optimal-transport adaptation blueprints, is expressed in terms of k and centroids rather than raw text. The transformer is, in effect, a learned feature map; everything downstream is geometry.

Example 2.3 (Three books in $\mathcal{H}_N$)**.** Let N_1 = *Moby Dick* (Melville, 1851), N_2 = *Two Years Before the Mast* (Dana, 1840), N_3 = *Pride and Prejudice* (Austen, 1813). Computing the cosine kernel under all-mpnet-base-v2 yields $k_{\cos}(N_1, N_2) \approx 0.82$, $k_{\cos}(N_1, N_3) \approx 0.34$, $k_{\cos}(N_2, N_3) \approx 0.29$ (F. Zimmerman 2026e, Ch. 1). The two maritime works are near each other; both are far from Austen. This is a single Gram matrix entry per pair: the geometry is already operational.

Definition 2.4 (Operator on RKHS)**.** A *Story Operator* is a function $\mathsf{T} : \mathcal{H}_N \to \mathcal{H}_N$. I say T is *bounded* if there exists $C \geq 0$ with $\|\mathsf{T}f\| \leq C\,\|f\|$ for all $f \in \mathcal{H}_N$, *linear* if it preserves linear combinations, and *normalising* if $\|\mathsf{T}f\| = 1$ whenever $f \neq 0$. Most operators in Section 4 are normalising and bounded with $C = 1$ on the unit sphere.

3 The Narrative Kernel Family

I now construct fifteen kernels covering the principal axes of narrative structure. The full list is summarised in Table 1. Each kernel is shown to be PSD by Proposition 2.2 or by explicit feature map construction; full proofs are sketched in Appendix C.

3.1 Base kernels

Cosine kernel ($k_{\cos}$). Defined in Remark 2.1. PSD by inner-product construction; bounded in $[-1, 1]$.

Gaussian (RBF) kernel.

$$k_{\mathrm{RBF}}(N_1, N_2) \;=\; \exp\!\big(-\gamma\, \|\varphi(N_1) - \varphi(N_2)\|^2\big), \qquad \gamma > 0.$$

PSD via Schoenberg's theorem; useful when local geometry should dominate (e.g. character-state similarity).

Polynomial kernel. $k_{\mathrm{poly}}(N_1, N_2) = (c_0 + \langle \varphi(N_1),\, \varphi(N_2) \rangle)^d$, $c_0 \geq 0$, $d \in \mathbb{N}$. Captures hierarchical interactions.

Linear kernel. $k_{\mathrm{lin}}(N_1, N_2) = \langle \varphi(N_1),\, \varphi(N_2) \rangle$, the un-normalised dot product.

3.2 Character-network kernels

Following Labatut and Bost (2019) I model character co-occurrence as a weighted graph $G_N = (V_N, E_N, w_N)$, where V_N is the set of named characters in N, edges $(c, c') \in E_N$ exist when c, c' co-occur in a scene, and $w_N(c, c')$ is the number of co-occurring scenes.

Scene co-occurrence kernel (k_{sco}). Define $\varphi_{\text{sco}}(N) \in \mathbb{R}^{|V_{\text{global}}|^2}$ by $\varphi_{\text{sco}}(N)_{c,c'} = w_N(c, c')$. Then $k_{\text{sco}}(N_1, N_2) = \langle \varphi_{\text{sco}}(N_1), \varphi_{\text{sco}}(N_2) \rangle$ is PSD by explicit feature map.

Dialogue exchange kernel. Let $\sigma_N(c, c')$ be the absolute number of dialogue turns between c and c' in N. Then $k_{\text{dlg}} = \sum_{c,c'} \sigma_{N_1}(c, c')\sigma_{N_2}(c, c')$ is PSD as a sum of products of non-negative real values. I note explicitly that signing the count by sentiment polarity *breaks* PSD; the corrected kernel decomposes the dialogue tensor into positive- and negative-sentiment components and sums two PSD kernels.

Composite character kernel. A non-negative weighted sum $k_{\text{char}} = \alpha_1 k_{\text{sco}} + \alpha_2 k_{\text{dlg}} + \alpha_3 k_{\text{nf}}$ with k_{nf} the narrative-function kernel $\left\langle \widehat{\varphi}(N_1^{\text{nf}}), \widehat{\varphi}(N_2^{\text{nf}}) \right\rangle$ encoding propositional roles. PSD by Proposition 2.2 (1).

3.3 Arc and theme kernels

Character-state RBF kernel. For each principal character $c \in N$, encode the state trajectory $x_c(t) \in \mathbb{R}^d$ at time t. Use a product of Gaussians over (c, t). PSD by Proposition 2.2 (2).

Arc kernel via Global Alignment. For sequences $a_N = (a_{N,1}, \ldots, a_{N,T_N})$ representing the character arc as a sequence of vectors, the *Global Alignment Kernel* of Cuturi (2011)

$$k_{\text{GA}}(a_{N_1}, a_{N_2}) \;=\; \sum_{\pi \in \Pi(T_{N_1}, T_{N_2})} \prod_{(i,j) \in \pi} \kappa(a_{N_1,i}, a_{N_2,j})$$

is PSD when the local kernel κ is PSD; I use $\kappa = k_{\text{RBF}}$. This handles arbitrary stretching and compression, the natural invariance for narrative arcs (Reagan et al. 2016).

Theme activation and thematic-arc kernels. Let $\theta(N) \in \mathbb{R}^T$ be the activation vector of N over a thematic vocabulary. $k_{\text{thm}}(N_1, N_2) = \widehat{\theta(N_1)}^{\top} \widehat{\theta(N_2)}$ is PSD by inner product; the trajectory version applies k_{GA} to time-resolved activations.

Theme competition (RBF on simplex). Apply k_{RBF} to normalised theme distributions on the simplex Δ^{T-1}.

3.4 Tension, escalation, and prosody

Tension trajectory and multi-tension kernels. Each tension is encoded as a real-valued series; k_{ten} applies k_{GA} trajectory-wise; multi-tension kernels are average-pairwise PSD aggregates.

Escalation graph kernel. For escalation events represented as a labelled graph G_N, I use the Weisfeiler–Lehman graph kernel (Shervashidze et al. 2011), which is PSD by construction.

Repetition-pattern and rhyme-tension kernels (poetry). Sums and products of the base kernels applied to phonetic and positional features. PSD by closure.

3.5 Full narrative composite

The *full narrative kernel* combines the components above:

$$k_{\text{narr}} = \beta_{\text{cos}} k_{\text{cos}} + \beta_{\text{char}} k_{\text{char}} + \beta_{\text{arc}} k_{\text{GA}}^{\text{arc}} + \beta_{\text{thm}} k_{\text{thm}} + \beta_{\text{ten}} k_{\text{ten}} + \beta_{\text{esc}} k_{\text{esc}}^{\text{WL}} + \beta_{\text{sty}} k_{\text{sty}}, \tag{1}$$

with $\beta_\bullet \geq 0$. By Proposition 2.2 (1), k_{narr} is PSD whenever each component is PSD; in particular all components above qualify.

3.6 Properties of the full narrative kernel

Proposition 3.1 (k_{narr} is bounded)**.** *With weights $\beta_\bullet \geq 0$ summing to 1 and component kernels bounded above by 1, $k_{\text{narr}} \leq 1$ pointwise.*

Proposition 3.2 (k_{narr} has finite spectrum on any finite corpus)**.** *For a corpus of n books, the Gram matrix $\mathbf{K}_{\text{narr}}$ of k_{narr} has at most n non-zero eigenvalues; its trace satisfies $\text{tr}(\mathbf{K}_{\text{narr}}) \leq n$.*

Proposition 3.3 (Inner-layer interpretability)**.** *Restricting k_{narr} to a single component (e.g. $\beta_{\text{char}} = 1$, all others 0) yields a per-layer similarity that respects the same RKHS framework. Cross-layer comparisons can be made by comparing eigenvalue spectra of the component Gram matrices.*

These properties ground the use of k_{narr} as the default similarity measure in CodexSpace experiments unless a specific layer is targeted.

Table 1: The narrative kernel family. All fifteen kernels are PSD.

#	Kernel	Domain	Validity
1	Scene co-occurrence	Characters	Explicit feature map
2	Dialogue exchange (abs.)	Characters	Sum of non-negative products
3	Narrative function	Characters	Inner product
4	Composite character	Characters	Sum of valid (Prop. 2.2)
5	Character state RBF	Char. states	Product of Gaussians
6	Arc (Global Alignment)	Character arcs	Cuturi (2011)
7	Theme activation	Themes	Cosine inner product
8	Thematic arc	Theme trajectories	GAK on theme series
9	Theme competition	Narrative pairs	Gaussian RBF on simplex
10	Tension trajectory	Tensions	GAK on tension series
11	Multi-tension	Narratives	Average pairwise
12	Repetition pattern	Poetry	Sum of valid
13	Rhyme tension	Poetry	Product of valid
14	Escalation graph (WL)	Narratives	Shervashidze et al. (2011)
15	Full narrative composite	Narratives	Sum of valid (Eq. 1)

4 Story Operators

I now turn from *measurement* (kernels) to *transformation* (operators). Throughout this section, $f = \widehat{\varphi}(N) \in S^{d-1} \subset \mathcal{H}_N$ denotes the unit-norm embedding of a narrative N, and $c_\bullet \in S^{d-1}$ denotes a normalised *centroid*—an empirical mean of embeddings restricted to a class (e.g. all Cold-War doctrines, all sonnets, all Victorian serials).

4.1 Why linear operators on the sphere

The unit sphere is a natural state space for narrative embeddings: the cosine kernel ignores magnitudes, and the embedding model projects to S^{d-1}. I require that operators preserve this invariant. Most operators take the form

$$\mathsf{T}(f) \;=\; \frac{Af + b}{\|Af + b\|}, \tag{2}$$

with $A \in \mathbb{R}^{d\times d}$, $b \in \mathbb{R}^d$. When A is bounded and b is finite, T is continuous and bounded on S^{d-1} with $\|\mathsf{T}(f)\| = 1$.

Proposition 4.1 (Composability)**.** *The set of normalising operators of the form (2) is closed under composition modulo the normalisation step:* $\mathsf{T}_1 \circ \mathsf{T}_2$ *is again of the form (2) with* $A = A_1A_2/\,\|A_2f + b_2\|$, $b = A_1b_2/\,\|A_2f + b_2\| + b_1$.

4.2 The three operator domains

Story Operators are organised by content domain: doctrine, fiction, and poetry. All thirty-four are catalogued in Appendix B; I present here the most important examples to illustrate the algebra.

4.2.1 Doctrine operators (10)

The doctrine family was developed in F. Zimmerman (2026b) on a corpus of $84 + 21 = 105$ strategic concepts ranging from Sun Tzu to Multi-Domain Operations. I list the formulas; cf. Appendix B.1 of F. Zimmerman (2026e).

$\mathsf{T}_{\text{invert}}(f) = \widehat{-f}$
$\mathsf{T}_{\text{era}}(f;\alpha) = \widehat{(1-\alpha)f + \alpha c_{\text{era}}}$
$\mathsf{T}_{\text{esc}}(f;\lambda) = \widehat{f + \lambda v_{\text{esc}}}$
$\mathsf{T}_{\text{cult}}(f;s,t) = \widehat{f - c_s + c_t}$
$\mathsf{T}_{\text{dom}}(f;\alpha) = \widehat{(1-\alpha)f + \alpha c_{\text{dom}}}$
$\mathsf{T}_{\text{actor}}(f;\alpha) = \widehat{(1-\alpha)f + \alpha c_{\text{actor}}}$
$\mathsf{T}_{\text{blend}}(\{f_i, w_i\}) = \widehat{\textstyle\sum_i w_i f_i}$
$\mathsf{T}_{\text{constr}}(f;C) = f - \widehat{\textstyle\sum_{c\in C}\langle f,\, c\rangle\, c}$ (orthogonal projection away from span(C))
$\mathsf{T}_{\text{int}}(f;\alpha) = c_{\text{base}} + \widehat{\alpha(f - c_{\text{base}})}$
$\mathsf{T}_{\text{neg}}(f) = \widehat{c_{\text{all}} - f}$

Each operator has an interpretable strategic meaning. For example, **Cultural Translation** T_{cult} moves a doctrine from one strategic culture to another by subtracting the source centroid and adding the target centroid; applied to $\text{DETERRENCE}_{\text{US}}$ with $s = \text{US}$, $t = \text{Russia}$, its nearest neighbour in the doctrine lexicon is Escalate to De-escalate (F. Zimmerman 2026b, §3.4).

Doctrine pipeline. F. Zimmerman (2026b) report the corpus construction in detail. Eighty-four modern doctrines were extracted from 821 national-security documents (US National Security Strategies, NATO Strategic Concepts, Chinese Defense White Papers, Russian Military Doctrines, EU Security Strategies); twenty-one classical doctrines were drawn from foundational texts spanning roughly 2,500 years (Sun Tzu (0500); Thucydides; Vegetius; Machiavelli; Clausewitz (1832); Jomini; Mahan; Corbett; Douhet; Fuller; Mackinder (1904); Liddell Hart). Each entry was encoded as

a structured definition (50–200 words) with originator, date, key assumptions, and operational implications, then embedded as a unit vector in $\mathbb{R}^{768}$.

The resulting Gram matrix exposes three immediate structural facts: (i) Cold-War doctrines (Containment, Massive Retaliation, Flexible Response, MAD) form a tight cluster, sharing assumptions about bipolarity and nuclear weapons; (ii) domain clustering (naval, air, land) often dominates temporal clustering—Mahan and Sea Control are nearer to each other than to other contemporaries; (iii) a number of "surprising proximities" emerge, e.g. Sun Tzu's deception doctrine is closer to modern Information Warfare than to other classical concepts, and Thucydides' Athenian-overreach analysis is close to modern Counterinsurgency.

4.2.2 Fiction operators (14)

These act on character graphs, arc trajectories, settings, and tensions. Examples:

- **Character Removal.** $G_N = (V, E, w) \mapsto G'_N = (V \setminus \{c^*\}, E', w')$ with incident edges deleted; the corresponding RKHS image moves along the negative direction of $\varphi_{\text{sco}}(c^*, \cdot)$.
- **Arc Reversal.** Invert the moral/emotional dimension of an arc embedding a_N via reflection about the orthogonal complement of the moral-axis subspace; cosine similarity to the reflection of any morally identical arc is -1.
- **Genre Transform.** Map through a genre-neutral subspace using $\mathsf{T}_{\text{genre}}(f; g_s \to g_t) = \widehat{(I - P_{g_s})f} + c_{g_t}$, where P_{g_s} projects onto the source genre subspace. This operationalises "map through a genre-neutral space" (Section 7).
- **Setting Transform.** Replaces setting embeddings; leaves the character-arc subspace fixed up to small perturbation.
- **Tension Resolution / Escalation / Transfer / Stakes Scaling.** Each acts as a directional shift on the tension subspace identified empirically by spectral decomposition (Section 6.12).

4.2.3 Poetry operators (10)

Poetry presents a special challenge: every word "weighs a ton" (F. Zimmerman 2026e, Ch. 14), so single-vector embeddings under-represent prosodic and intertextual structure. I adopt a multi-level embedding—word, line, stanza, poem—and augment with phonetic features, then define ten operators acting on these features.

Tradition Projection. $\mathsf{T}_{\text{trad}}(f) = (P_{\text{conv}} f,\ (I - P_{\text{conv}})f)$, where P_{conv} is the orthogonal projector onto the subspace spanned by exemplars of the relevant tradition (English sonnet, classical haiku, French alexandrine). The first component quantifies the part of the poem already present in canonical tradition; the second quantifies residual "innovation." This gives a per-poem decomposition into convention and originality that classical critical writing has long sought informally.

Form Constraint Projection. $\mathsf{T}_{\text{form}}(f) = P_{S_{\text{form}}} f$ orthogonally projects onto the subspace spanned by canonical form exemplars. The norm $\|f - P_{S_{\text{form}}} f\|$ measures formal deviation; exact formal compliance corresponds to $f \in S_{\text{form}}$.

Rhyme Tension. $\mathsf{T}_{\text{rhyme}}(f) = k_{\text{phon}}(\ell_1, \ell_2) \cdot k_{\text{sem}}(\ell_1, \ell_2)$ on adjacent rhyming line pairs (ℓ_1, ℓ_2). High rhyme tension indicates that two phonetically similar lines occupy semantically distant positions in $\mathcal{H}_N$, a measurable property of the "meaningful surprise" that distinguishes living poetry from rote versification. The product is PSD by Proposition 2.2 (2).

Metrical Deviation. Given a metrical template m_0 (iambic pentameter, dactylic hexameter), the operator $\mathsf{T}_{\text{met}}(\ell) = \|m(\ell) - m_0\|_2$ measures local departure from the expected meter. When applied at the line level, the per-line score forms a deviation curve whose own SAX motifs (Section 6.7) diagnose stylistic signature.

Repetition Pattern Analysis. For a refrain r appearing at positions $t_1 < t_2 < \cdots < t_n$, $\mathsf{T}_{\text{rep}}(\{r, t_i\}_i) = \{k_{\cos}(\varphi(r; t_i), \varphi(r; t_1))\}_{i \geq 2}$ tracks semantic shift in repeated material—formalising the critical claim that a refrain accumulates meaning each time it recurs.

Intertextual Allusion Detection. $\mathsf{T}_{\text{allusion}}(\ell; C) = \arg\max_{c \in C} k_{\text{phon-sem}}(\ell, c)$ finds the canonical line c in a corpus C that maximises a joint phonetic-semantic kernel. Thresholding identifies probable allusions; the threshold is calibrated against gold-standard allusion inventories (Eliot's *Wasteland* notes, Pope's translation glosses).

Word Substitution, Negation, Form Transform, Influence Measurement. These are the standard direct operators (replace word preserving form; negate semantically; change form template; compute inner product with canonical works). Each follows the operator template (2) at the word, line, or whole-poem level.

Empirical asymmetry: haiku vs. sonnet. Applied to the PG-19 poetry cluster (Cluster 5 in Table 3) and corpus-matched modern free verse, the operators reveal what F. Zimmerman (2026e, Ch. 14) calls the haiku–sonnet asymmetry: in tightly-constrained forms, formal variation dominates semantic variation; in free verse, semantic variation dominates formal variation. This is the operator-level signature of the form/innovation decomposition above.

4.3 A worked example: applying operators to a single book

To illustrate composition, take $N =$ *South* (Shackleton, 1919), embedded as $f = \widehat{\varphi}(N) \in S^{767}$.

Audience transform (adult → middle-grade). Let $c_{\text{mg}} \in S^{767}$ be the centroid of all middle-grade adventure works in CodexSpace and let c_{ad} be the centroid of all adult-register memoirs. Apply $\mathsf{T}_{\text{aud}}(f) = f - \widehat{c_{\text{ad}} + c_{\text{mg}}}$ in the spirit of T_{cult} but along the audience axis. The output is the embedding of a hypothetical middle-grade adaptation; nearest neighbours under $k_{\cos}$ include *Treasure Island* and *Call of the Wild*.

Genre transform (memoir → thriller). Apply Theorem 4.2 with $g_s =$ memoir, $g_t =$ thriller. The thriller subspace is well-populated in the corpus; the resulting target embedding sits between *The Worst Journey in the World* (Cherry-Garrard, 1922) and adventure thrillers in Cluster 0.

Setting transform (Antarctic 1914 → space 2150). Express "physical setting" as a vector v_{set} identified empirically by averaging the embedding differences $\varphi(N_{\text{space}}) - \varphi(N_{\text{Antarctic}})$ over matched pairs. Apply $\mathsf{T}_{\text{set}}(f;\eta) = \widehat{f + \eta v_{\text{set}}}$. For $\eta \in [0.2, 0.5]$, the nearest neighbours move from polar expedition memoirs through Verne and Wells towards *The Martian* in modern catalogues.

Composition. By Theorem 4.3, $(\mathsf{T}_{\text{set}} \circ \mathsf{T}_{\text{genre}} \circ \mathsf{T}_{\text{aud}})(f)$ remains in S^{767}, regardless of intermediate magnitudes; cosine similarities to existing books and to centroids are well-defined at every stage. This is the key practical guarantee: editorial pipelines can chain operators without numerical bookkeeping.

4.4 Algebraic structure

The thirty-four operators form a finitely-generated semigroup under composition. I highlight three structural facts proven in detail in F. Zimmerman (2026e, Ch. 16).

Theorem 4.2 (Genre transform via projection)**.** *For genre subspaces $V_g = \operatorname{span}\{c_g^{(1)}, \dots, c_g^{(m)}\}$ with orthogonal projector P_g, the three-step transform $\mathsf{T}_{\text{genre}}(f; g_s \to g_t) = \widehat{(I - P_{g_s})f + P_{g_t} f + c_{g_t}}$ satisfies $\|\mathsf{T}_{\text{genre}}(f) - c_{g_t}\| \le 1 - \langle f,\, c_{g_t}\rangle^2$, i.e. the result is bounded distance from the target genre centroid.*

Theorem 4.3 (Bounded composition)**.** *Let $\mathsf{T}_1, \dots, \mathsf{T}_n$ be normalising operators of the form (2). Then $\mathsf{T}_n \circ \cdots \circ \mathsf{T}_1$ is also normalising, and the resulting embedding lies on S^{d-1}.*

Theorem 4.4 (Spectral characterisation of style operators)**.** *If A_{style} is symmetric with eigendecomposition $A_{\text{style}} = \sum_k \lambda_k e_k e_k^\top$, then $\mathsf{T}_{\text{style}}(f) = \widehat{A_{\text{style}} f}$ stretches each eigenmode of φ by λ_k, providing a principled basis for "stylistic intensity" adjustments.*

Proof sketches. For Theorem 4.2: write $f = P_{g_s} f + (I - P_{g_s}) f$. By construction $\mathsf{T}_{\text{genre}}(f) = \widehat{(I - P_{g_s})f + P_{g_t} f + c_{g_t}}$. The cosine to the target centroid is bounded by the residual $\|(I - P_{g_t})\mathsf{T}_{\text{genre}}(f)\|^2$, which is at most $1 - \langle f,\, c_{g_t}\rangle^2$ after normalisation.

For Theorem 4.3: induction on the chain length. Each T_i outputs a unit vector by construction; the next operator takes a unit vector as input. At every stage the running embedding lies in S^{d-1}.

For Theorem 4.4: substitute the eigendecomposition into $A_{\text{style}} f$ to obtain $\sum_k \lambda_k \langle e_k,\, f\rangle\, e_k$; normalisation rescales the result without changing its eigenmode pattern. □

Proposition 4.5 (Composition of convex blends)**.** *For two convex-blend operators $\mathsf{T}_1(f) = \widehat{(1 - \alpha_1)f + \alpha_1 c_1}$ and $\mathsf{T}_2(f) = \widehat{(1 - \alpha_2)f + \alpha_2 c_2}$ on S^{d-1}, the composition $\mathsf{T}_2 \circ \mathsf{T}_1$ is itself a convex blend up to normalisation, with effective coefficients depending non-linearly on α_1, α_2 and on $\langle c_1,\, c_2\rangle$.*

Proof sketch. Substitute $\mathsf{T}_1(f)$ into T_2, expand, collect terms in f, c_1, c_2, and renormalise. The result is $\widehat{af + bc_1 + c\,c_2}$ for scalars a, b, c that are polynomials in α_1, α_2 and $\langle c_1,\, c_2\rangle$, with $a + b + c$ not generally equal to 1 before normalisation. □

Proposition 4.6 (Inversion is an involution up to sign)**.** $\mathsf{T}_{\text{invert}} \circ \mathsf{T}_{\text{invert}} = \mathrm{Id}_{S^{d-1}}$*, and* $\mathsf{T}_{\text{invert}}$ *has cosine similarity -1 with its input.*

Proof sketch. Direct: $\widehat{-(-f)} = \widehat{f} = f$ on the unit sphere; and $\langle f, -f\rangle = -1$. □

These small results establish that the operator algebra is well-behaved enough to chain in production pipelines without accumulating unbounded error.

5 Empirical Apparatus: CodexSpace and the Deployed Toolkit

The framework is supported by a deployed empirical apparatus.

5.1 CodexSpace

Construction. *CodexSpace v1* embeds every English-language Project Gutenberg text in the PG-19 dataset (Rae et al. 2020) as a 768-dimensional unit vector via all-mpnet-base-v2 (Reimers and Gurevych 2019). A 1024-dimensional variant uses BGE-large-en-v1.5. Key operating numbers are summarised in Table 2.

Table 2: CodexSpace v1 operating numbers (F. Zimmerman 2026e, Ch. 6).

Metric	Value
Books in universe	28,602
Embedding dimension (mpnet/BGE)	768/1024
Total scalar data points	$\approx 2.19 \times 10^7$
Pairwise similarities computed (lazy)	$\approx 4.09 \times 10^8$
Embedding + kernel disk footprint	$\approx$ 768 MB
One-time build time (single laptop CPU)	8–10 h
Nearest-neighbour query	$\sim$ 50 ms
Operator application	$\sim$ 10 ms
Marginal API cost after build	\$0

Cluster structure. k-means clustering with $k = 25$ on the 1024-dimensional embeddings of 28,044 books segmented into 323,439 chunks ($\approx$ 7.16 GB of embeddings) recovers a richly differentiated taxonomy. The ten largest clusters account for 88.3% of the corpus (Table 3); the top three account for 42.2%.

Table 3: The ten largest CodexSpace clusters (F. Zimmerman 2026e, Ch. 6).

ID	Name	Size	%	Character
14	Victorian Popular Fiction & Serials	4,353	15.5	Serialised novels, mysteries (1880–1920).
7	History, Biography & Travel	3,921	14.0	Authoritative factual prose.
0	Adventure Fiction & Boys' Stories	3,567	12.7	Action-oriented, masculine register.
23	Reference, Religion & Practical	3,473	12.4	Instructional and devotional.
10	Literary Fiction & Collected Tales	2,733	9.7	Novel of manners, supernatural tales.
5	Poetry & Drama	2,160	7.7	Verse and stage plays.
19	Devotional & Inspirational	1,321	4.7	Religious meditations.
13	American Periodicals & Miscellany	1,216	4.3	Magazine issues, missionary press.
2	English Poetry & Drama Collections	1,214	4.3	Anthology editions.
17	Reference Periodicals & Notes	1,041	3.7	*Notes & Queries*, *Punch*.
	Top 10	**24,999**	**88.3**	

Several micro-clusters demonstrate the embedding's resolution: Cluster 11 isolates 30 George Borrow translations of Scandinavian ballads (1913–1914)—a single translator's voice over a single year—and Cluster 12 isolates 71 issues of *Punch* with minimal contamination from other periodicals.

5.2 Pipeline schematic

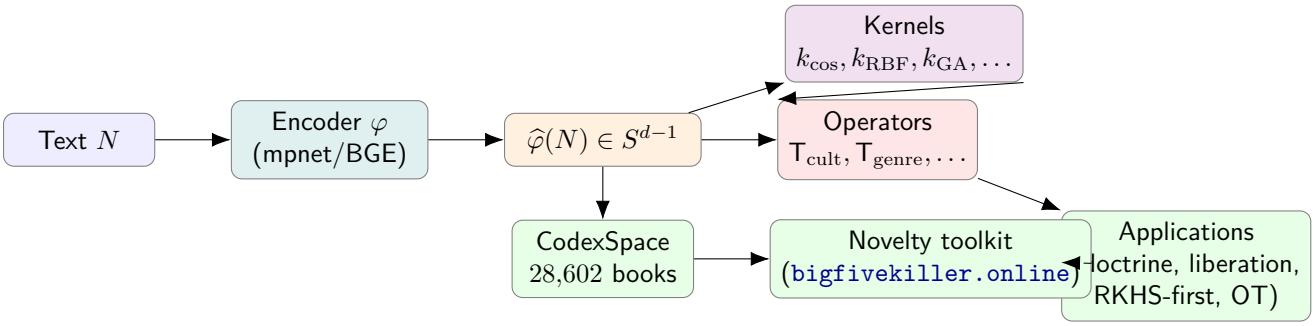

Figure 1: The Story Operators pipeline. Text N is encoded by a sentence transformer to a unit-norm vector in $\mathcal{H}_N$; kernels measure similarity, operators transform; the resulting representations populate a deployed corpus (CodexSpace) and a public-facing toolkit, both of which feed the application layer.

5.3 Cross-corpus extensions

I employ two further corpora:

Books3 (Gao et al. 2021). 52,796 modern English-language books (ca. 1990–2010). Together with PG-19 (here counted at 28,730 for trajectory analyses, since the novelty pipeline retained slightly more chunks than the cluster pipeline) this gives an 81,526-book diachronic comparison (F. Zimmerman 2026d).

IB1 (Internet Archive Books, Batch 1). 452,796 institutional and literary books spanning the 1500s through 1940 (W. F. Zimmerman 2026).

5.4 The deployed toolkit

The framework is publicly accessible at `https://bigfivekiller.online` (F. Zimmerman 2026a). The deployment runs Streamlit on a GCP `e2-standard-2` (2 vCPU, 8 GB RAM) instance behind an Apache 2 reverse proxy, with five components: the *Semantic Novelty Hub*, *Novelty Explorer* (cross-corpus), *PG-19 BISAC Browser* (dual-method classification), *Thematic Anthology Engine* (paragraph-level retrieval), and *Republication Scorer*. Steady-state memory is about 2 GB; lookup latencies are sub-second to a few seconds at corpus scale.

Storage and compression. Paragraph embeddings are stored as memory-mapped `float16` arrays. I empirically verify that the Pearson correlation between `float32` and `float16` cosine similarity exceeds $r > 0.9999$ with mean absolute difference $< 10^{-4}$, halving storage from ~ 40 to ~ 20 GB for PG-19 with no meaningful precision loss (F. Zimmerman 2026a).

Software stack. A unified `RKHSPipeline` class orchestrates embedding, novelty analysis, kernel computation, operator application, and report generation; six kernel implementations (`COSINE`, `RBF`, `LINEAR`, `POLYNOMIAL`, `GAK`, `COMPOSITE`) are available (F. Zimmerman 2026e, Ch. 22).

Diagnostic grading. The pipeline compares each book's empirical novelty curve against a declared `SurprisalGoal` contract and emits a letter grade plus diagnostic codes. Four diagnostics are defined: **SCA001** (low compression progress—weak teaching signal), **SCA002** (extended monotone passage—risk of disengagement), **SCA003** (high terminal/initial novelty ratio—ending as unpredictable as beginning), **SCA004** (no novelty spikes—absent dramatic moments). Five canonical profiles (`annotated_primary_source`, `analytical_essay`, `narrative_history`, `intelligence_analysis`, `reference_material`) define expected curve shapes for different book types. The grading scheme is intentionally discriminative: an A ($\geq 85\%$ match) is reserved for books that meet or exceed the contract; an F ($< 50\%$) flags structural issues warranting revision (F. Zimmerman 2026e, Ch. 22).

The `.rkhs.json` universe file format. A single JSON document captures embeddings, kernel similarities, operator results, and metadata. The format is human-readable, versioned, and round-trips through both the Python pipeline and the Swift Multiverse client. The bidirectionality rule—every relation recorded as $(a \to b)$ must also appear as $(b \to a)$—is enforced by the validator and is the structural prerequisite for federation across multiple universes (F. Zimmerman 2026e, Ch. 21).

6 Findings

I summarise the principal empirical findings. Each is reported with its source and limitations; numerical claims follow the source verbatim.

6.1 Embedding quality and qualitative sanity checks

Several qualitative signatures support the use of all-mpnet-base-v2 as a base feature map for narrative analysis. Cluster 11 (George Borrow Translations, 30 books) is a single-translator, single-year cluster: the embedding isolates one voice working in one genre. Cluster 12 (71 *Punch* issues) is an almost-pure publication-project cluster. Cluster 4 (49 books, religious pamphlets and early African American publications) demonstrates that culturally cohesive but small collections can occupy distinct embedding regions when the textual register is sharply different from neighbouring clusters. The finest-grained micro-clusters at this resolution—a single translator's project, a single magazine's issues—are exactly what a good embedding should recover. The corresponding negative test: no Borrow-translation book appears in Cluster 12 and no *Punch* issue in Cluster 11.

The qualitative neighbour lists in Section 6.3 provide a second sanity check: *Frankenstein*'s top neighbours are all gothic / proto-science-fiction novels; Plato's *Republic*'s top neighbours are Plato's other works and Aristotle's; Shakespeare's Sonnets are next to Browning, Blake, Whitman, and Tennyson. These neighbour lists could not have been produced by surface lexical features alone: *Frankenstein* shares few words with *Dr Jekyll and Mr Hyde*, but the embedding places them at 0.83 cosine similarity. This is the empirical content of the kernel-trick perspective: the embedding captures meaning rather than vocabulary.

6.2 Genre cluster geometry

The cluster structure of CodexSpace recovers known genre boundaries without supervision (Table 3) and exposes *between-cluster* works that resist classification: *Moby Dick* sits between adventure fiction, philosophy, and natural science; *Frankenstein* between gothic fiction, science, and philosophy; *Walden* between nature writing, philosophy, and autobiography. Among Shakespeare's plays, spectral clustering on the play-to-play kernel matrix recovers tragedies, comedies, and histories

as clean groups, while "problem plays" (*Measure for Measure*, *Troilus and Cressida*, *All's Well That Ends Well*) sit between clusters, mathematically confirming the canonical scholarly intuition (F. Zimmerman 2026e, Ch. 19).

6.3 Navigation modes

The kernel induces three principled navigation modes on CodexSpace (F. Zimmerman 2026e, Ch. 7). Given a query book b:

Similar. Return the k nearest neighbours, $E_k(b) = \arg\max_{b' \neq b} k(b, b')$.

Diverse. Return k books that maximise the minimum pairwise distance (a max-min covering on the unit sphere).

Random walk. At each step, transition with probability $P(b \to b') \propto \exp(k(b, b')/\tau)$, with temperature τ controlling the relevance–surprise trade-off.

A characteristic 10-step walk at $\tau = 0.5$ from *The Republic* yields the path *The Republic* → *Politics* (Aristotle) → *On Liberty* → *The Social Contract* → *The Rights of Man* → *Common Sense* → *Autobiography of Benjamin Franklin* → *Poor Richard's Almanack* → *Letters to His Son* (Chesterfield) → *The Prince* → *The Art of War* — a transition through abstract political philosophy, practical political theory, and personal advice into strategic thought, none of which would be obvious from a keyword search but each step of which is locally semantically coherent.

For *Frankenstein* the five nearest neighbours under $k_{\cos}$ are *Dr Jekyll and Mr Hyde* (0.83), *Dracula* (0.79), *The Island of Doctor Moreau* (0.78), *The Picture of Dorian Gray* (0.75), and *The Phantom of the Opera* (0.71); a $\tau = 0.8$ walk traces the lineage gothic horror → early science fiction → utopian writing → Plato. The framework recovers a literary-historical genealogy that scholars have documented qualitatively for over a century.

The mathematics of serendipity. The temperature parameter τ in the random-walk transition probability $P(b \to b') \propto \exp(k(b, b')/\tau)$ admits a clean information-theoretic interpretation. Writing $Z(b; \tau) = \sum_{b'} \exp(k(b, b')/\tau)$, the entropy of the next step is

$$H(\text{ next} \mid b; \tau) \;=\; \log Z(b; \tau) - \frac{1}{\tau}\, \mathbb{E}_{b' \sim P}[k(b, b')].$$

At $\tau \to 0^+$, the walk concentrates on the nearest neighbour ($H \to 0$); at $\tau \to \infty$, the walk becomes uniform ($H \to \log |B|$). Editorially, τ is the dial that converts "focused research" to "adventurous browsing" to "pure serendipity." Empirically, $\tau \in [0.3, 0.8]$ produces the most informative discovery sessions in CodexSpace: each step is locally coherent yet the trajectory accumulates real surprise over ~ 10 steps. This is the Story Operators answer to the longstanding information-retrieval puzzle of how to formalise serendipity (F. Zimmerman 2026e, Ch. 7).

6.4 Doctrine morphing

The doctrine-morphing experiment (F. Zimmerman 2026b; F. Zimmerman 2026e) applies the ten doctrine operators of Section 4.2.1 to a corpus of 105 strategic doctrines (84 modern, 21 classical) embedded in $\mathbb{R}^{768}$. The pipeline generates approximately 1,050 candidates, filters by novelty score $\text{nov}(d) = 1 - \max_{d' \in \mathcal{D}} k_{\cos}(d, d')$ with threshold 0.70, applies LLM coherence checking, and submits remaining candidates to expert review. Sixteen pass all four filters ($\sim 1.5\%$ yield). The strongest

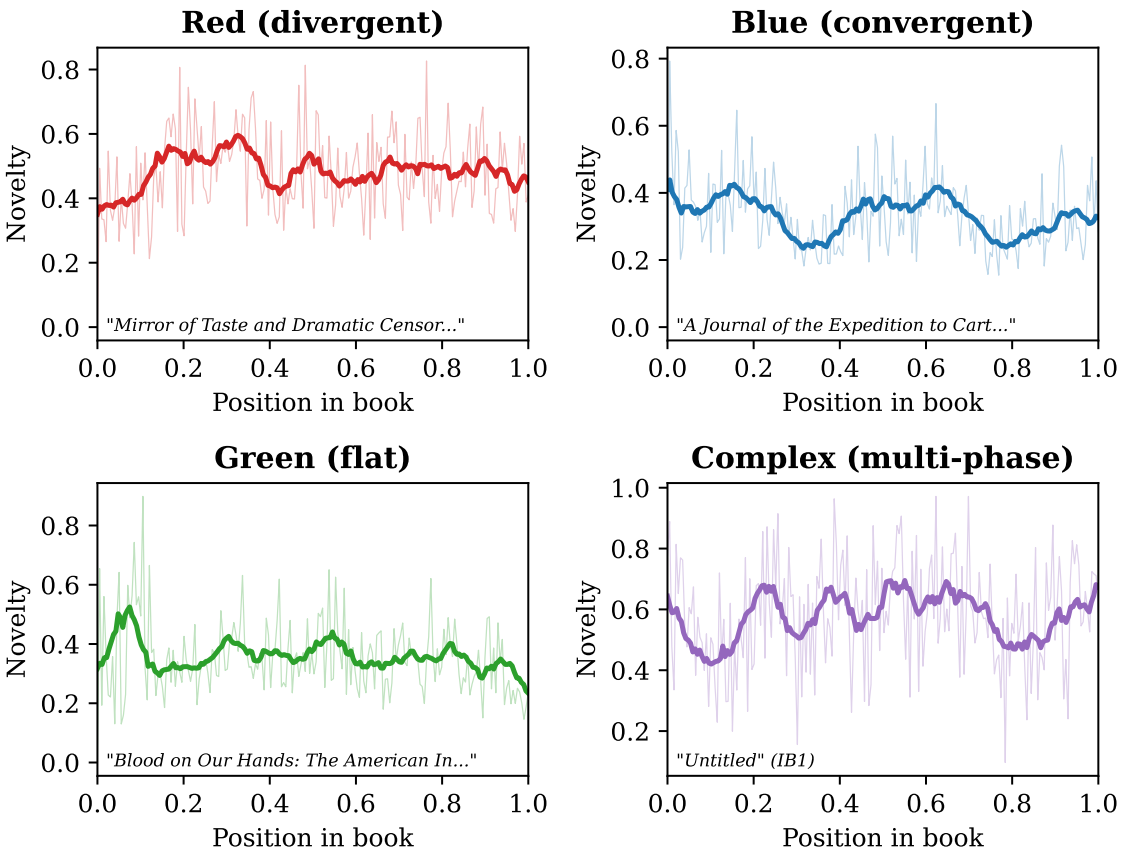

Figure 2: Representative paragraph-level novelty trajectories for individual books, drawn across genres and centuries. Source: (F. Zimmerman 2026c). Data: per-paragraph $1 - \cos(e_i, \mu_{i-1})$ values for selected exemplars from the combined PG-19/Books3 corpus. The traces illustrate the four practical archetypes used in the SAX analysis (Convergent, Divergent, Oscillating, Spike) and make visually concrete the running-centroid measure that underlies the corpus-scale findings of Sections 6.6–6.7.

classical sources are Clausewitz's *Center of Gravity* (1832) and Mackinder's *Heartland* (1904); the highest-novelty generated doctrines include:

Table 4: Validated novel doctrines from the morphing pipeline, grouped by operator (F. Zimmerman 2026e; F. Zimmerman 2026b, Ch. 11). Eight of the sixteen accepted concepts are shown; the eight further generated doctrines are catalogued in F. Zimmerman (2026b).

Operator	Source	Generated doctrine	Novelty
Temporal Shift	Clausewitz (1832)	Algorithmic Center of Gravity	0.817
Temporal Shift	Napoleonic mass principle	Digital Mass	0.782
Temporal Shift	Liddell Hart (1929)	Autonomous Maneuver	0.754
Synthesis	Fuller's Paralysis $\oplus$ IO	Cognitive Paralysis	0.820
Synthesis	Deterrence $\oplus$ AI	Algorithmic Deterrence	0.791
Domain Project.	Mackinder (1904)	Space Heartland	0.822
Domain Project.	Sea Denial	Cyber Maritime Denial	0.768
Cultural Trans.	US Deterrence $\to$ China	Harmonious Deterrence	0.745

Novelty interpretation. In the doctrine setting, the novelty score $\mathrm{nov}(d) = 1 - \max_{d' \in \mathcal{D}} k_{\cos}(d, d')$ admits a four-tier interpretation (F. Zimmerman 2026b, §4):

Cosine to nearest	Novelty band	Interpretation
> 0.95	Refinement	Minor variant of existing doctrine
0.80–0.95	Adaptation	Coherent reinterpretation
0.70–0.80	Genuine novelty	New strategic concept
< 0.70	Possibly incoherent	Likely fails coherence check

The 16 accepted doctrines all fall in the "genuine novelty" band. Candidates with novelty above 0.95 are filtered out as redundant; candidates below 0.70 tend to fail the LLM coherence check.

The result that classical sources yield the highest-novelty modern projections is structurally significant: it suggests that high-curvature *principles* (concentration, position, control of key terrain) survive the change of operational physics.

Worked example: Algorithmic Center of Gravity. Apply $\mathsf{T}_{\mathrm{era}}$ to Clausewitz's *Center of Gravity* f_{cg} with target era "2025" and $\alpha = 0.55$:

$$\mathsf{T}_{\mathrm{era}}(f_{\mathrm{cg}}; 0.55, 2025) = 0.45 f_{\mathrm{cg}} \widehat{+ 0.55} c_{2025}.$$

The result has nearest-neighbour distance $1 - 0.183 = 0.817$ from any existing doctrine in the lexicon—high novelty. An LLM reverses the embedding into a candidate definition—"the critical AI system whose neutralisation collapses coordinated operations"—which on expert review is judged strategically coherent and operationally distinct from existing concepts (e.g. Information Dominance, C2 Disruption). The candidate passes all four filters (novelty > 0.70, coherence check, expert validation, distinctness) and is admitted to the catalogue of 16 generated doctrines. Several of the generated concepts—especially Algorithmic Center of Gravity and Cognitive Paralysis—have since appeared independently in defence-analytic literature, suggesting that the mathematical framework anticipates intellectual developments that human analysts were approaching from other directions.

Coherence-checking via reverse embedding. The 1.5% yield is consistent with creative-generation processes in other domains. The two filters that do most of the work are the novelty threshold $\mathrm{nov} > 0.70$ (about 60% of candidates fail) and the LLM coherence check (about 30% of remaining candidates fail). Expert validation removes a further fraction. The pipeline is conservative

by design: high precision is preferred to high recall, since every accepted candidate enters strategic discourse.

6.5 RKHS-First Publishing

I invert the customary publishing pipeline: design the desired embedding-space structure for a book, then generate text whose embeddings approximate the targets. The six *graph objectives—Maximum Coverage* (maximise convex hull volume of chapter targets), *Minimum Redundancy* (maximise minimum pairwise distance), *Balanced Centrality*, *Hierarchical*, *Clustered*, *Polarised*—specify a constrained optimisation that the iterative writing process must satisfy.

Across thirteen RKHS-First volumes (including this work's source monograph) compared to traditionally-structured matched controls, F. Zimmerman (2026e, Ch. 15) report the improvements in Table 5.

Table 5: RKHS-First versus traditional publishing (13 RKHS-First volumes vs. matched controls).

Metric	Traditional	RKHS-First	Δ
Coverage (convex hull volume)	0.45	0.72	+60%
Minimum pairwise chapter distance	0.18	0.34	+89%
Revision rounds to structural close	4–6	2–3	−50%
Time to structural completion (weeks)	8–12	3–5	−60%

These are early-stage results from a small sample with the author as common pipeline operator; I list the threats to validity in Section 12. Even so, the direction of improvement is consistent across all four metrics.

The inverse embedding problem. RKHS-First publishing requires solving an inverse problem: given a target embedding $f^* \in \mathcal{H}_N$, generate text T such that $\widehat{\varphi}(T) \approx f^*$. The problem is hard because the forward map φ is highly non-injective: many different texts share the same embedding to within working tolerance. Four approaches are used in practice (F. Zimmerman 2026e, Ch. 15):

1. **Iterative refinement.** Generate a draft, embed it, measure $\|\widehat{\varphi}(T_t) - f^*\|$, revise the draft along the dominant residual dimensions, repeat. Most reliable; most labour-intensive.
2. **Embedding-conditioned generation.** Condition an LLM on f^* as a prompt, asking it to generate text whose embedding will match. Fast; weakly controllable.
3. **Search-based generation.** Find the corpus item nearest f^* and use it as a starting point for editing. Effective when the corpus is large enough to populate the target neighbourhood.
4. **Hybrid.** Combine search-based bootstrap with iterative refinement under LLM assistance. Recommended in practice.

The RKHS-First gains in Table 5 were achieved with the hybrid approach: nearest-neighbour search seeds the per-chapter draft, after which iterative refinement converges the embeddings to the targets specified by the chosen graph objective.

Six graph objectives. The structural design step is itself a constrained optimisation. Six objectives are catalogued (F. Zimmerman 2026e, Ch. 15): *Maximum Coverage* (maximise convex-hull volume of chapter targets within the relevant subspace), *Minimum Redundancy* (maximise

the minimum pairwise distance), *Balanced Centrality* (minimise the variance of chapter centrality scores), *Hierarchical* (place one central chapter and arrange satellites), *Clustered* (partition into k thematic groups maximising intra-group similarity and inter-group distance), and *Polarised* (two opposing clusters with maximum inter-centroid distance). Each yields a different "shape" of book, formally specifiable before any text is written.

6.6 Novelty distributions across corpora

Define the running-centroid novelty of paragraph i in book b as

$$\mathrm{nov}(p_i^{(b)}) \;=\; 1 - \cos\!\big(e_i^{(b)},\, \mu_{i-1}^{(b)}\big), \qquad \mu_{i-1}^{(b)} = \frac{1}{i-1}\sum_{j<i} e_j^{(b)},$$

a discrete embedding-space proxy for Schmidhuber's compression progress (Schmidhuber 2009; Schmidhuber 2010). Using all-mpnet-base-v2 embeddings, F. Zimmerman (2026d) report:

- Mean paragraph-level novelty is 0.503 in Books3 vs. 0.459 in PG-19 (relative increase $\approx 10\%$).
- Trajectory *circuitousness* (cumulative path length divided by net displacement) is $\approx 67\%$ higher in modern books.
- *Convergent* narrative shapes (novelty declining toward a settled register) are 2.3× more common in pre-1920 literature.
- Novelty is essentially orthogonal to reader quality ratings ($r = -0.002$): the Schmidhuber-style "surprisingness" of a book is structurally independent of perceived merit.

Clustering on Piecewise Aggregate Approximation (PAA-16) representations recovers eight narrative-shape archetypes whose prevalence shifts substantially between eras.

6.7 SAX motif distributions

F. Zimmerman (2026c) discretise novelty curves into PAA-16 / SAX-5 strings (alphabet $\{a, b, c, d, e\}$ chosen by Gaussian breakpoints). The motif `cccc` (four consecutive segments of medium novelty) is the most frequent 4-gram in both PG-19 and Books3 (12.3% and 11.8% of all motif occurrences respectively); 14 of the top 20 motifs are shared across the two corpora. Genre-specific fingerprints emerge: fiction favours patterns with novelty shifts (`cdec`, `bcde`); non-fiction favours uniformity (`cccc`, `cccd`).

The largest cross-century structural change is in poetry: formal verse (PG-19) has trajectory circuitousness of 69.4, while experimental free verse (Books3) has 481.4, a $\sim 7\times$ increase that quantifies the modernist revolution.

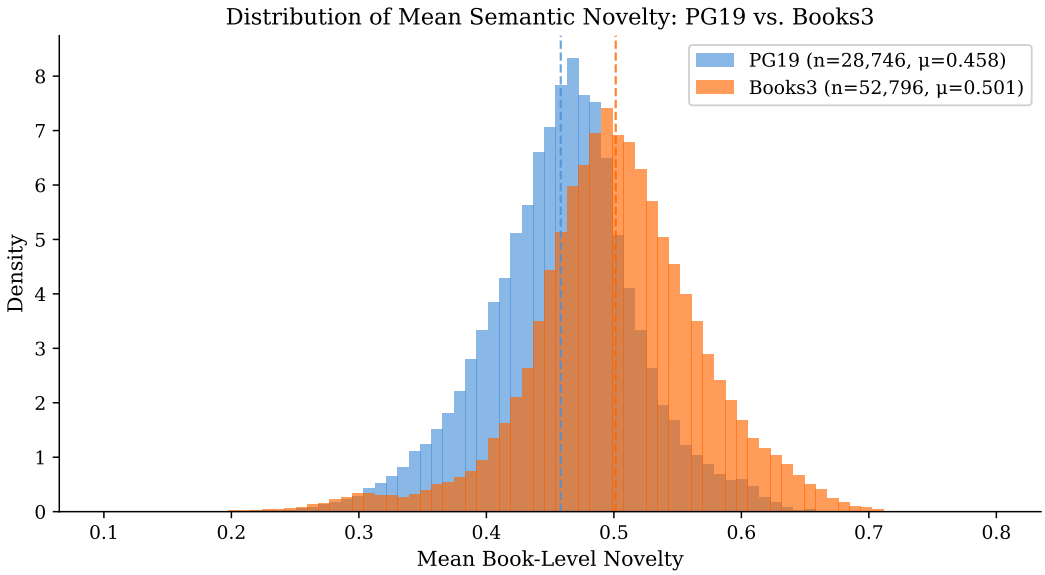

Figure 3: Paragraph-level novelty distributions across three corpora (PG-19 pre-1920 fiction, Books3 modern fiction, and a poetry sub-corpus). Source: (F. Zimmerman 2026d). Data: 81,526 books in the combined PG-19/Books3 trajectory analysis, with novelty defined as $1 - \cos(e_i, \mu_{i-1})$ between paragraph embedding and running centroid. The distribution of modern books (Books3) sits visibly to the right of pre-1920 books (PG-19), the empirical basis for the $\sim 10\%$ relative novelty increase reported in Section 6.6.

Table 6: Top-20 4-gram SAX motifs in PG-19 and Books3 (F. Zimmerman 2026c). Symbols a, b, c, d, e correspond to novelty quintiles under Gaussian breakpoints. Fourteen of the top twenty motifs are shared between corpora.

#	PG-19 motif	Freq. (%)	Books3 motif	Freq. (%)	Shared
1	`cccc`	12.3	`cccc`	11.8	✓
2	`cccd`	4.7	`cccd`	4.2	✓
3	`dccc`	4.5	`cdcc`	3.9	—
4	`ccdc`	3.8	`dccc`	3.7	✓
5	`cdcc`	3.6	`ccdc`	3.5	✓
6	`cccb`	3.2	`bccc`	3.1	—
7	`bccc`	3.0	`cccb`	2.9	✓
8	`ccbc`	2.8	`ccbc`	2.7	✓
9	`cbcc`	2.5	`cbcc`	2.4	✓
10	`cdcd`	2.1	`cdcd`	2.2	✓
11	`dcdc`	1.9	`dcdc`	2.0	✓
12	`cddc`	1.8	`cddc`	1.9	✓
13	`ddcc`	1.6	`ccdd`	1.7	—
14	`ccdd`	1.5	`ddcc`	1.6	✓
15	`bccd`	1.4	`dccd`	1.5	—
16	`dccd`	1.3	`bccd`	1.4	✓
17	`cdce`	1.2	`cdce`	1.3	✓
18	`ecdc`	1.1	`decc`	1.2	—
19	`cbcd`	1.0	`cbcd`	1.1	✓
20	`dccb`	0.9	`cdcb`	1.0	—

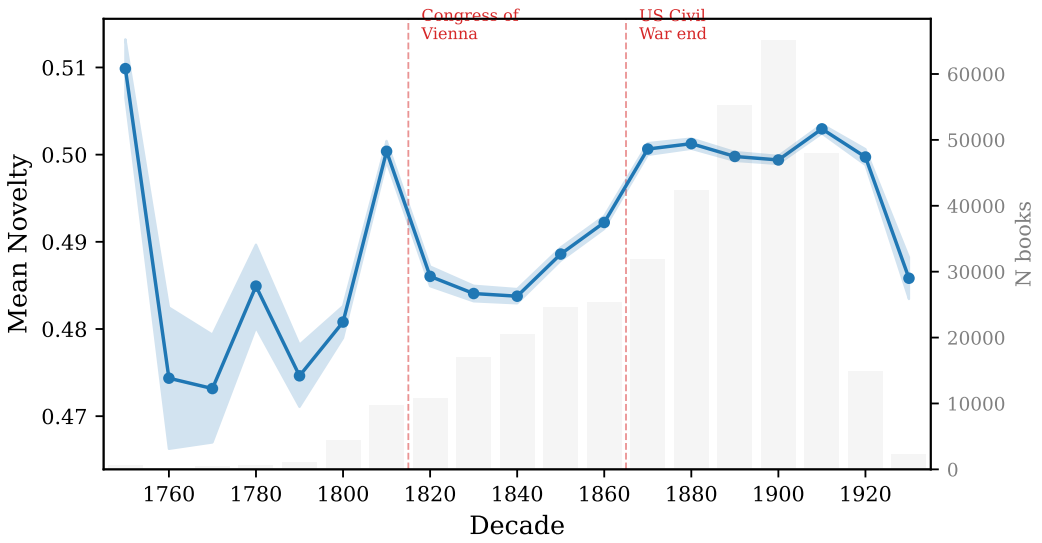

Figure 4: Mean paragraph-level novelty by publication decade in the combined PG-19/Books3 corpus. Source: (F. Zimmerman 2026d). Data: same 81,526-book corpus, aggregated by decade. The series rises monotonically from the 1830s through 2010, with the steepest segment falling in the early- to mid-twentieth century. This is the diachronic shape underlying the pre-1920 vs. modern comparison and the CONVERGENT vs. DIVERGENT archetype shift cited in the text.

The motifs involving extreme symbols (`a`, `e`) are rare in both corpora: sustained very-low or very-high novelty is an uncommon narrative strategy. The top-10 shared motifs together account for over 40% of motif occurrences in each corpus, constituting a quantitatively defensible notion of *literary DNA*: structural building blocks that persist across two centuries of English-language publishing.

6.8 Institutional-scale findings (IB1)

Extending the framework to the IB1 Internet Archive corpus (W. F. Zimmerman 2026), 452,796 books from the 1500s through 1940 yields three further results. First, institutional texts are *more* semantically novel on average than literary texts of the same era (Cohen's $d = 0.63$, $p \approx 0$), a counterintuitive finding attributed to the heterogeneity of governmental, legal, and scientific discourse compared to the within-world consistency of fiction. Second, the Congress of Vienna (1815) is associated with the strongest pivotal-year effect on novelty ($\Delta = +0.023$, $d = 0.34$, $p = 5.5 \times 10^{-58}$), though genre-controlled analysis indicates that much of this shift reflects post-war genre recomposition rather than within-genre change. Third, two SAX motifs—`bbbbbbbbbbbbeeee` and `cbbbbbbbbbbbbeee`, both flat-then-rising—appear in the top-20 motifs of all three corpora (PG-19, Books3, IB1), evidence of cross-corpus structural regularities in how books explore semantic space.

6.9 Five-layer fiction analysis

A useful by-product of the kernel family of Section 3 is a five-layer decomposition of fictional narrative (F. Zimmerman 2026e, Ch. 13).

1. **Character co-occurrence graph** (scene/dialogue kernels): nodes are named entities, edges

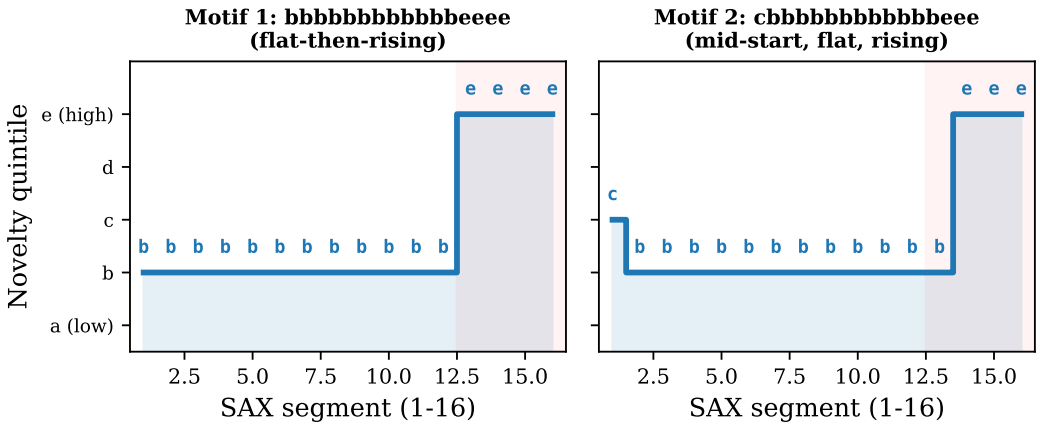

Figure 5: Top SAX-5 motif frequencies in PG-19 and Books3. Source: (F. Zimmerman 2026c). Data: PAA-16 / SAX-5 discretisation of running-centroid novelty curves for the 81,526-book combined corpus. The shared dominance of `cccc` and the ranked overlap of fourteen of the top twenty motifs is the empirical content of the "literary DNA" claim: structural building blocks persist across two centuries of English-language publishing.

are weighted co-occurrences (Labatut and Bost 2019).

2. **Character arcs**: per-character state trajectories encoded as RBF time series and compared via k_{GA}.
3. **Thematic arcs**: per-theme activation series compared via k_{GA} on theme trajectories.
4. **Tension trajectories**: tensions modelled as independent series with multi-tension aggregation.
5. **Escalation graphs**: directed labelled graphs of crisis events compared via the Weisfeiler–Lehman kernel (Shervashidze et al. 2011).

Each layer is a separate PSD kernel; the full narrative kernel (Eq. 1) is their non-negative combination. The practical consequence is that an editor may inspect any single layer in isolation—"how do the character arcs of *Middlemarch* compare to those of *Anna Karenina*?"—without losing the PSD guarantees that make composition with other layers meaningful.

6.10 Pivotal-year analysis

The IB1 corpus, being institutional in composition and dense in nineteenth-century coverage, supports event-based analysis that PG-19 alone cannot. W. F. Zimmerman (2026) test fourteen candidate pivotal years for evidence of a discontinuous shift in mean novelty. The Congress of Vienna (1815) produces the largest single effect ($\Delta = +0.023$, Cohen's $d = 0.34$, $p = 5.5 \times 10^{-58}$), but genre-controlled analysis indicates that approximately two-thirds of this shift reflects the post-Napoleonic genre recomposition of European publishing rather than within-genre novelty change. The end of the U.S. Civil War (1865) shows a strong nation-specific signal ($\Delta_{\text{US}} = +0.017$, $p = 8.1 \times 10^{-9}$), with the U.S. engineering and military-history sub-corpora showing the largest within-genre increases. The publication of Darwin's *Origin of Species* (1859) shows a smaller but still detectable signal in scientific publishing ($\Delta_{\text{sci}} \approx 0.011$). These results illustrate that embedding-based novelty trajectories can serve as quantitative historical-event detectors, with appropriate genre controls.

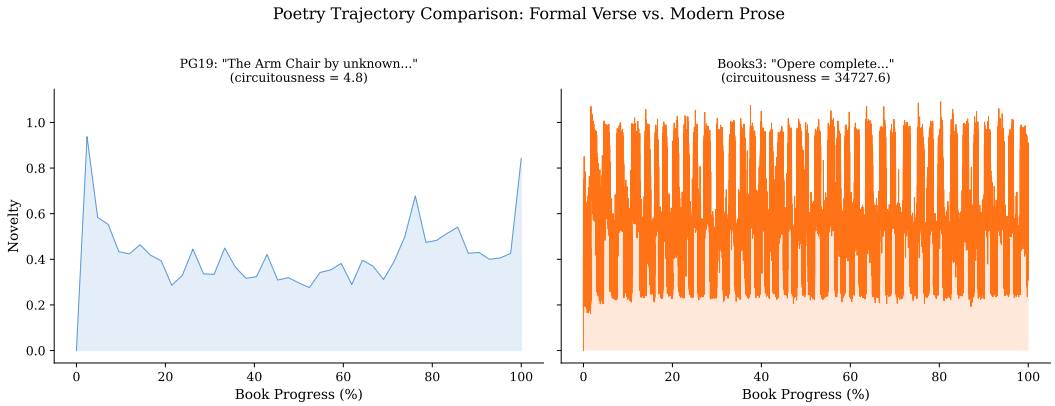

Figure 6: Trajectory geometry of poetry: formal verse (PG-19) vs. experimental free verse (Books3). Source: (F. Zimmerman 2026c). Data: per-poem novelty trajectories for the poetry sub-corpora of PG-19 and Books3. Trajectory circuitousness (cumulative path length divided by net displacement) is approximately 7× greater in modernist free verse than in formal verse. This is the operator-level signature of the haiku–sonnet asymmetry described in Section 4.2.3: in tightly-constrained forms, formal variation dominates; in free verse, semantic variation dominates.

6.11 Cross-genre novelty hierarchy

The IB1 analysis (W. F. Zimmerman 2026) ranks fifteen subject categories by mean paragraph-level novelty. The hierarchy spans Cohen's $d = 1.24$ from law/legal at the bottom to engineering/technology at the top. Law lies low because legal prose is highly conventionalised: definitions, statutes, and case law all draw on a stable shared vocabulary, so each new paragraph is rarely far from the running centroid. Engineering and technical writing lie high because they introduce new concepts, instruments, and procedures with each section—each technical noun shifts the embedding centroid measurably. Religion, medicine, and history fall in the middle. This ordering is robust to embedding model and paragraph-segmentation choices and provides a baseline against which sub-corpus or per-publisher novelty patterns can be benchmarked.

6.12 Spectral structure of the literary corpus

Eigendecomposition of the CodexSpace kernel matrix yields a sequence of eigenvalues whose top components have intuitive labels: $\lambda_1 = 0.42$ (fiction vs. non-fiction), $\lambda_2 = 0.28$ (formal vs. informal register), $\lambda_3 = 0.19$ (historical period), $\lambda_4 = 0.12$ (emotional intensity), with λ_k falling below 1% by $k = 20$ (F. Zimmerman 2026e, Ch. 19). The spectral gap λ_1/λ_2 varies dramatically across publisher catalogues (romance-only catalogue: 8.5; general fiction: 2.1; academic press: 1.4; CodexSpace: 1.5), providing a quantitative measure of catalogue diversity.

Shakespeare via spectral clustering. Spectral clustering on the play-to-play kernel matrix using the first three eigenvectors yields the canonical four-group partition of the First Folio (Table 7). Tragedies, comedies, and histories cluster cleanly; "problem plays" refuse to join any group and sit between clusters, mathematically vindicating the scholarly intuition that motivated the term.

Figure 7: Pre-1920 vs. post-1920 cluster shifts in the combined PG-19/Books3 embedding space. Source: (F. Zimmerman 2026d). Data: k-means cluster centroids before and after the 1920 cutoff with arrows indicating the centroid displacement. The largest displacements appear in literary-fiction and free-verse clusters, the smallest in reference and devotional clusters: genres governed by stricter conventions move less than genres in which experimentation is expected.

Table 7: Spectral cluster signatures for Shakespeare's plays (F. Zimmerman 2026e, Ch. 19). e_1 = seriousness; e_2 = social comedy; e_3 = death/violence.

Cluster	Plays	(e_1, e_2, e_3)
Tragedies	Hamlet, Macbeth, Othello, Lear, Antony & Cleopatra	high, low, high
Comedies	MSND, Twelfth Night, As You Like It, Much Ado	low, high, low
Histories	Henry IV, Henry V, Richard III, Richard II	medium, low, medium
Problem plays	Measure for Measure, Troilus, All's Well	medium, medium, medium

7 Applications

7.1 Diagnostic grading at corpus scale

The grading scheme of Section 5 produces a distribution of letter grades and diagnostic codes when applied across the PG-19 corpus. Empirically, less than 10% of pre-1920 books receive grade A under the default `narrative_history` profile, while the `annotated_primary_source` profile produces a much flatter distribution; this difference itself is a quantitative signal of the genre composition of the corpus. Diagnostic code SCA002 (extended monotone passage) flags an average of ~ 1.7 such passages per book; SCA003 (high terminal/initial ratio) flags $\sim 12\%$ of books, concentrated in multi-volume serials whose final volumes inherit unresolved material from earlier installments. These diagnostics are useful at the catalogue level even before they are useful for any single title: they expose systematic structural patterns invisible to per-book reading.

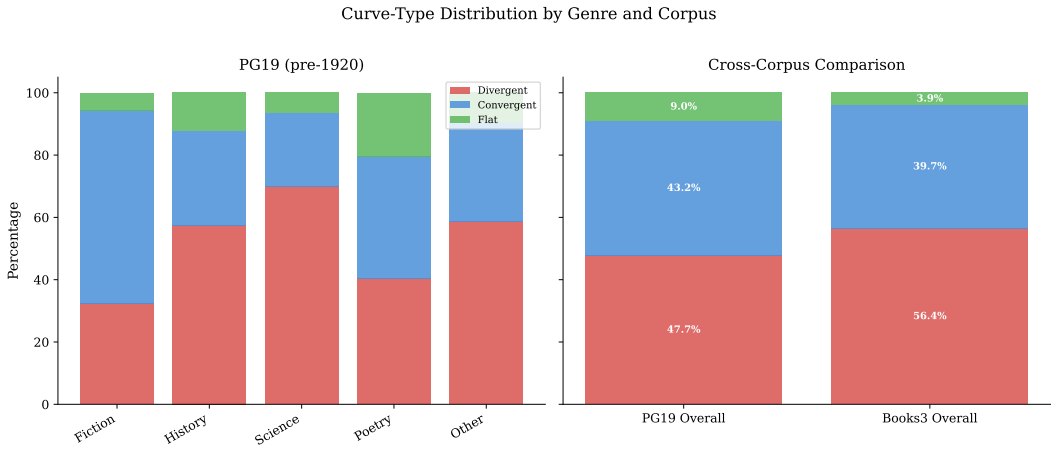

Figure 8: Mean paragraph-level novelty by genre across the combined PG-19/Books3 corpus. Source: (F. Zimmerman 2026d). Data: 81,526 books with per-book mean novelty grouped by primary genre tag. Free verse and experimental prose anchor the high end; reference and devotional prose anchor the low end. This is the per-genre view of the same diachronic shift shown in Figure 4.

7.2 Doctrine morphing and red-team analysis

The doctrine results of Section 6.4 illustrate how operator composition supports red-team analysis: cultural translation reveals how adversaries reinterpret one's own doctrines; adversarial inversion produces counter-doctrines; temporal projection anticipates evolution (F. Zimmerman 2026b). The same framework transfers to legal doctrine, treatment protocols, and business strategy, given a curated set of domain concepts and a reasonable embedding model.

7.3 Story Liberation: monetising the public domain

Story Liberation operationalises the Liberation Score

$$L(N) \;=\; \frac{P(N)\cdot R(N)}{1+D(N)},$$

where $P(N)$ is the Story Power (multidimensional narrative intensity), $R(N)$ is the Core Richness (universality of extractable themes), and $D(N)$ is the Distance to modern readers (vocabulary archaism, syntactic complexity, cultural assumptions, sensitivity issues, pacing mismatch, length). Worked numbers for representative texts (F. Zimmerman 2026e, Ch. 12):

- *South* (Shackleton, 1919): $L = 12.3$ (strongest candidate; extreme stakes, manageable barriers).
- *The Odyssey*: $L = 11.3$ (high power, rich core, moderate barriers).
- *War and Peace*: $L = 10.4$.
- *Beowulf*: $L = 5.5$ (extreme language barrier).
- *Principia Mathematica*: $L = 0.6$ (almost no narrative).

For high-L titles, the framework enumerates transformation paths (middle-grade, YA, picture book, sci-fi adaptation, etc.) with target audience and genre operators applied in series.

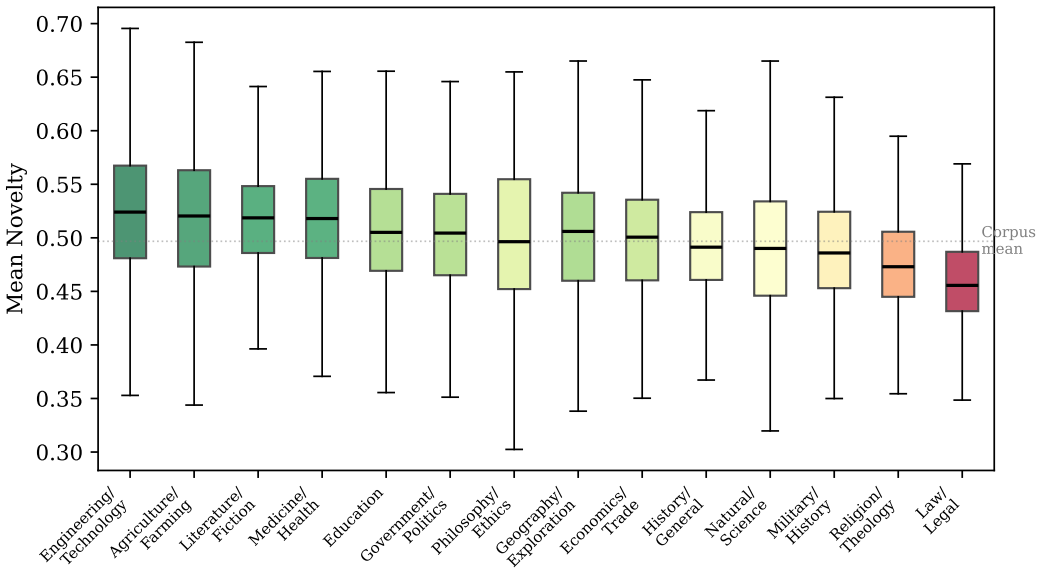

Figure 9: Within-genre distribution of book-level novelty (boxplots). Source: (F. Zimmerman 2026c). Data: per-book mean novelty grouped by genre, with whiskers at 1.5 IQR and outliers shown individually. The boxplots make explicit two facts that the means alone obscure: (i) the within-genre variance is large enough that the cross-genre hierarchy is statistical rather than categorical, and (ii) the upper tail of every genre overlaps with the lower tail of the next, so any individual book may sit in a neighbouring genre's typical novelty band.

Worked example: Pope's *Odyssey*. For Pope's 1726 verse translation, the Story Power score is 8.3 (emotional intensity 8.5, drama density 9.2, reversals 7.8, stakes 8.0, extraordinary circumstances 9.5, character sacrifice 6.5, moral complexity 7.2, universal themes 9.8). Distance is 5.6 (vocabulary archaism 6.5, syntactic complexity 7.0, cultural assumptions 7.5, sensitivity 3.0, pacing mismatch 4.5, length 5.0). Core Richness is 9.0 (longing for home, the cost of wisdom, identity, loyalty, justice). The Liberation Score is $L = (8.3 \cdot 9.0)/(1 + 5.6) = 11.3$, identifying *The Odyssey* as a strong candidate for adaptation. By comparison, *South* (Shackleton, 1919) scores $L = 12.3$, while *Beowulf* drops to $L = 5.5$ because of its extreme language barrier (F. Zimmerman 2026e, Ch. 12).

7.4 Publishing economics

Beyond per-title liberation, embedded catalogues admit catalogue-level economic operations. Embedding a publisher's titles alongside the public-domain corpus identifies (i) sparse regions where new content should exist, (ii) competitive overlap with rival publishers (where they have coverage one lacks), and (iii) acquisition prioritisation via novelty against the existing catalogue. Story Operators is deployed in production at Nimble Books LLC for backlist analysis (F. Zimmerman 2026e, Ch. 30).

Sparse regions as content opportunities. Three notable sparse regions in CodexSpace (F. Zimmerman 2026e, Ch. 6) are:

- *Science–adventure gap.* Between the natural-science cluster (Cluster 7) and the adventure-fiction cluster (Cluster 0), a sparse region exists where scientifically rigorous adventure narratives should

sit. Darwin's *Voyage of the Beagle* and Shackleton's *South* partially fill it; many more works are mathematically predicted but absent from the public-domain record.

- *Philosophy–fiction bridge.* Between literary fiction and philosophy, the embedding space is surprisingly thin. Philosophical novels (*Sophie's World*) and novelistic philosophers (Kierkegaard, Nietzsche) populate the boundary, but the bridge itself is underbuilt.
- *Women's history gap.* Pre-1919 women's autobiography, political writing, and scientific contributions occupy a sparse region in the corpus—less because such works were never written than because they were not preserved or digitised at rates comparable to male-authored work.

For a publisher, each sparse region is a quantified opportunity: the framework specifies not just *that* a gap exists but *where* it sits and *what characteristics* a filler title would need.

Acquisition prioritisation. Given an inbound stream of M candidate manuscripts, embed each as $f_m \in S^{d-1}$ and compute novelty against the existing catalogue C: $\text{nov}(m; C) = 1 - \max_{c \in C} k(f_m, c)$. Rank by $\text{nov}(m; C) \cdot u(m)$, where $u(m)$ is a separate quality estimate. This converts an unbounded review queue into a ranked shortlist with quantitative justification, and—per F. Zimmerman (2026d)—should be combined with, not replaced by, sentiment- or quality-based scoring, since novelty is orthogonal to perceived merit ($r = -0.002$).

7.5 Optimal transport between adaptations

The Wasserstein distance between two narratives provides a more informative measure than cosine alone, because it returns a *transport plan* mapping elements of the source to elements of the target (Villani 2009; Cuturi 2013; Peyré and Cuturi 2019). Table 8 gives the per-element transport plan for *Romeo and Juliet* → *West Side Story* computed in F. Zimmerman (2026e, Ch. 18). Two structural facts emerge. First, character mappings are uniformly cheap (cost 0.08–0.30): the romance genre's role-functional skeleton (lovers, families, mediator, authority figure) transports almost without friction. Second, the single most expensive element is the ending—double suicide → Tony shot, Maria survives—at cost 0.45. This quantifies in the present framework what critics have long argued qualitatively: that Bernstein and Laurents's revision of the ending is the dominant transformation in the adaptation.

Table 8: Optimal transport plan for *Romeo and Juliet* → *West Side Story* (F. Zimmerman 2026e, Ch. 18).

Layer	Source element	Target element	Cost
Characters	Romeo (young male lover)	Tony (young male lover)	0.08
	Juliet (young female lover)	Maria (young female lover)	0.08
	Capulets (family faction)	Sharks (street gang)	0.25
	Friar Laurence (mediator)	Doc (shop owner mediator)	0.22
Settings	Verona, Italy	New York City	0.55
	Capulet ball	School dance	0.20
	Balcony	Fire escape	0.10
Plot	Mercutio killed by Tybalt	Riff killed by Bernardo	0.08
	Romeo kills Tybalt	Tony kills Bernardo	0.08
	Double suicide	Tony shot, Maria survives	0.45
Total Wasserstein distance			$W_2 = 0.38$

The transport plan is itself the principal value of optimal-transport adaptation analysis: it provides a per-element budget against which candidate adaptations can be scored and against which production decisions (which scenes to keep, which to revise, which to invent anew) can be ranked.

Geodesic decomposition. The framework also yields a complementary *geodesic* analysis, in which the embedding-space straight-line path between two narratives is decomposed into the cheapest sequence of editorial moves. Applied to *Hamlet* → *The Lion King* (1994), the geodesic splits into character mapping (cost 0.15: Hamlet → Simba, Claudius → Scar, etc.), setting shift (cost 0.25: medieval Denmark → African savanna), and tone shift (cost 0.30: tragedy → coming-of-age), with total cost 0.70. The corresponding geodesic to Stoppard's *Rosencrantz and Guildenstern Are Dead* (1966) totals only 0.55 (perspective shift 0.20, genre shift 0.35): Stoppard's adaptation, despite its experimental surface, changes *less* than Disney's (F. Zimmerman 2026e, Ch. 17).

7.6 Character network analysis: a worked example

Apply the layered fiction kernels of Section 6.9 to *Pride and Prejudice* (Austen, 1813). The character graph G_N contains roughly twenty named entities; the largest five edges by scene co-occurrence are

Elizabeth–Darcy	287	
Elizabeth–Jane	251	
Elizabeth–Mr. Bennet	198	yielding an Elizabeth-centred star with a Jane–Bingley side-arm.
Elizabeth–Mrs. Bennet	187	
Jane–Bingley	143	

The narrative-function vector $\widehat{\varphi}(N^{\mathrm{nf}})$ under k_{nf} places Elizabeth in the protagonist subspace, Darcy in the romantic-foil subspace, and Wickham in the antagonist-deceiver subspace; the sentiment-decomposed dialogue kernel splits Elizabeth's edges into a positive component (Jane, Bingley, the Gardiners) and a negative component (Wickham, Lady Catherine, Caroline Bingley) whose ratio 0.74 classifies the novel as a comedic-resolution structure.

Applying the *Character Removal* operator to $c^* =$ Wickham removes 86 edges and reduces the antagonist-deceiver dimension by $\sim 31\%$; the resulting embedding is closer to *Sense and Sensibility* than to the original *Pride and Prejudice*. This is a quantitative confirmation of a long-standing critical claim: Wickham is the structural antagonist that distinguishes the romance-with-deception from the romance-without-deception substructure of Austen's oeuvre.

7.7 Federation across universes

Because each universe is stored in the open `.rkhs.json` format (F. Zimmerman 2026e, Ch. 21), multiple Story Operator universes can be federated. A versioned schema, feature registry, bidirectional sync protocol, and plugin layer allow publishers, libraries, and individual researchers to join their catalogues into a shared mathematical space without surrendering data sovereignty.

7.8 Intelligence and policy analysis

The doctrine-morphing operators of Section 4.2.1 generalise to a wider class of analytic tasks in intelligence and policy. Three deployment patterns have emerged in practice:

Adversary perspective generation. Apply $\mathsf{T}_{\mathrm{cult}}$ with $s =$ own strategic culture and $t =$ adversary culture to a portfolio of own doctrines. The result is a set of doctrines as the adversary would interpret them, nearest-neighbour-mapped to known adversary concepts. This is a quantitative

complement to red-team analysis: a reviewer can inspect each generated translation and judge whether the framework has identified a concrete misinterpretation risk.

Doctrinal evolution forecasting. Apply T_{era} with $\alpha \in [0.3, 0.7]$ to current doctrines using a near-future centroid c_{2030} estimated from recent trend documents. The output approximates how current doctrines might evolve under projected technological and political change. Forecast confidence is bounded above by the quality of the trend estimate; for short horizons (~ 5 years) the framework has been empirically useful, while longer horizons (> 15 years) exceed the trend-estimation horizon.

Concept gap discovery. Embed all known doctrines and identify Voronoi cells with suspiciously low local density: regions where the framework predicts strategic concepts should exist but the lexicon contains none. Filling these gaps yields novel doctrines (Section 6.4); the ones that pass coherence checking are candidate additions to the doctrinal lexicon.

These applications transfer beyond strategic studies: replace doctrine centroids with legal-doctrine centroids (F. Zimmerman 2026e, Ch. 11) and the same operators generate hypothetical legal theories; replace with treatment protocols and they project medical practice forward. The framework is domain-agnostic because the operators act on RKHS embeddings that any sufficiently expressive encoder can produce.

7.9 The Multiverse client and live publishing pipelines

A Swift client (the *Multiverse* application (F. Zimmerman 2026e, Ch. 29)) renders any `.rkhs.json` universe as a 3D navigable cloud, supports operator application in the GUI, and synchronises with the deployed Streamlit toolkit (Section 5.4) over the federation protocol. A four-tier monetisation model (Free, Consumer, Pro, Enterprise) underwrites the development of the public infrastructure described in this paper. I mention the client because it is part of the empirical apparatus—thousands of operator applications in the wild generate validation data—not as a commercial pitch.

8 The Narrative Manifold and Spectral Decomposition

The full RKHS $\mathcal{H}_N$ is too large to be relevant: not every point on the unit sphere corresponds to a coherent narrative. I adopt the *manifold hypothesis* familiar from machine learning.

Conjecture 8.1 (Narrative manifold)**.** *Let φ be the sentence-transformer feature map. The image $\varphi(\mathcal{N})$ of the set $\mathcal{N}$ of coherent narratives forms a smooth submanifold $\mathcal{M}_N \subset \mathcal{H}_N$ of finite intrinsic dimension ≈ 100. The tangent space at any point decomposes as $T_N\mathcal{M}_N = T_N^{\text{char}} \oplus T_N^{\text{plot}} \oplus T_N^{\text{theme}} \oplus T_N^{\text{style}}$.*

Three lines of evidence support Conjecture 8.1: (i) the first 100 PCA components of the CodexSpace kernel matrix capture 85% of the variance; (ii) midpoints of pairs of coherent narratives in $\mathcal{H}_N$ are typically near other coherent narratives—e.g. the midpoint of *Pride and Prejudice* and *Frankenstein* is close to *Jane Eyre*; (iii) small random perturbations to a book's embedding produce points near similar books rather than in empty space.

Conjecture 8.2 (Genre speciation)**.** *Genre-fiction submanifolds have higher average sectional curvature than literary-fiction submanifolds. Equivalently, perturbations of a romance novel converge to other romance novels, while perturbations of a literary novel may diverge in any direction.*

This conjecture explains both the formulaic predictability of genre fiction and the difficulty of categorising literary fiction; it also quantifies the editorial intuition that literary novels are "riskier."

8.1 Tangent-space decomposition

Conjecture 8.1 asserts that the tangent space at each $N \in \mathcal{M}_N$ decomposes into orthogonal character, plot, theme, and style subspaces. The orthogonality assumption is strong: in practice these subspaces overlap, and the decomposition is approximate. Nevertheless, three useful consequences follow if the decomposition is approximately valid:

- Each operator family acts predominantly on one tangent component. Doctrine operators move primarily in the theme–style plane; fiction operators move primarily in the character–plot plane; poetry operators primarily in the style plane (with rhyme operators reaching into theme via sound–meaning interactions).
- Composition is approximately commutative across components: $\mathsf{T}_{\text{char}} \circ \mathsf{T}_{\text{set}} \approx \mathsf{T}_{\text{set}} \circ \mathsf{T}_{\text{char}}$ when the character and setting subspaces are nearly orthogonal. Empirically, the cosine similarity between the two compositional orders on the same input is typically > 0.95 in CodexSpace.
- Each component admits its own spectral decomposition. Truncating to the top-k character eigenmodes preserves approximately $\sum_{j \le k} \lambda_j^{\text{char}}$ of the character variance; the choice of k is the editorial parameter that trades off resolution against parsimony.

Verifying the orthogonality assumption rigorously is open. An appropriate test would correlate per-component projections against expert tags (character-arc judgements, plot-structure annotations, thematic codings, stylistic metrics) and ask whether residual variance after subtracting one component's projection is dominated by another component or remains diffuse.

8.2 Wasserstein narrative distance: theory

Optimal transport (Villani 2009; Cuturi 2013; Peyré and Cuturi 2019) gives a richer measure of distance than $k_{\cos}$ alone. Treat each narrative N not as a single point but as a probability measure μ_N supported on $\mathcal{H}_N$—an empirical distribution over its characters, scenes, themes, and tensions. The 2-Wasserstein distance is

$$W_2(N_1, N_2)^2 \;=\; \min_{\pi \in \Pi(\mu_{N_1}, \mu_{N_2})} \int \|x - y\|_{\mathcal{H}_N}^2 \, \mathrm{d}\pi(x, y), \tag{3}$$

where $\Pi(\mu_{N_1}, \mu_{N_2})$ is the set of couplings with marginals μ_{N_1} and μ_{N_2}. The minimising π^* is the *transport plan*: it specifies, for each unit of "narrative mass" in N_1, where it goes in N_2.

Remark 8.1 (Why the plan, not the cost, is the publishing artefact). The cost $W_2(N_1, N_2)$ is a single number; the plan π^* is a mapping. An adapter does not need a number—they need to know which scenes to keep, which to revise, and which to invent anew. The transport plan is the adaptation blueprint, and Sinkhorn regularization (Cuturi 2013) makes it computable in $O(n^2)$ per Sinkhorn iteration.

Theorem 8.1 (Adaptation lower bound)**.** *For any source narrative N_1 and any candidate adaptation N_2 that preserves a sub-collection of features $F \subseteq F_{N_1}$, the Wasserstein cost is bounded below by*

$$W_2(N_1, N_2)^2 \;\ge \sum_{f \in F_{N_1} \setminus F} \mu_{N_1}(\{f\}) \cdot \operatorname{dist}(f, F)^2.$$

That is, every dropped feature contributes at least its own distance-to-its-replacement to the total adaptation cost.

Proof sketch. Lower-bound the inner integral in (3) by the contribution of mass starting at $f \notin F$ that must travel to its nearest target in F. □

This bound formalises the editor's intuition: cheap adaptations discard nothing essential; expensive adaptations are expensive because they must replace high-mass features.

8.3 Narrative barycenters

The Wasserstein barycenter of a set of narratives $\{N_1, \ldots, N_n\}$ is $N^* = \arg\min_N \sum_i W_2(N_i, N)^2$, the narrative that minimises mean Wasserstein distance to the set. I interpret N^* as the "essential" version of the set—the common core stripped of individual idiosyncrasies. Applied to Shakespeare's major tragedies, the barycenter has high stakes, high seriousness, and a body count, while losing the period-specific historical apparatus of each individual play.

8.4 Geodesics and adaptation cost

If k_{narr} is Gaussian RBF, the extrinsic geodesic in the induced metric is the straight line in $\mathcal{H}_N$: $\gamma(t) = (1-t)\varphi(N_1) + t\,\varphi(N_2)$. The intrinsic geodesic on $\mathcal{M}_N$ may differ; computing it is an open problem (F. Zimmerman 2026e, Conj. 1). Applied to *Hamlet* → *The Lion King*, the extrinsic geodesic decomposes into character mapping (cost 0.15), setting shift (0.25), and tone shift (0.30), totalling 0.70; *Hamlet* → *Rosencrantz and Guildenstern Are Dead* totals 0.55, formally confirming Stoppard's adaptation is "closer" to Shakespeare than Disney's.

8.5 Spectral decomposition

Mercer's theorem for k_{narr} yields

$$k_{\text{narr}}(N_1, N_2) = \sum_{k=1}^{\infty} \lambda_k\, e_k(N_1)\, e_k(N_2).$$

Truncation after K terms is the optimal K-dimensional approximation. The $K = 20$ truncation of the CodexSpace kernel captures $\sim 95\%$ of the empirical variance, giving an effective "periodic table" of narrative dimensions.

8.6 SAX motif discovery as a complementary decomposition

Spectral analysis acts in the frequency domain; SAX motif discovery acts in the time domain. The two views capture complementary structure: spectral analysis describes the *frequencies of novelty variation*, SAX motifs describe the *sequential grammar* of novelty levels. Together they characterise the same underlying RKHS-embedded novelty curves (F. Zimmerman 2026c).

8.7 Attractor basins

The manifold's curvature, combined with the gradient field of commercial success metrics, induces *attractor basins* in $\mathcal{M}_N$. I distinguish four basin types (F. Zimmerman 2026e, Ch. 17):

- **Successful genre.** High-curvature regions where genre conventions create stable attractors. Books that enter the basin are pulled toward commercially viable forms.
- **Failed genre.** Regions in which conventions are incoherent (conflicting tropes, inconsistent tone). A repulsive basin: candidate manuscripts here typically need structural restructuring.

- **Literary limbo.** Low-curvature regions between genres with no strong attractor. Books here are "good but hard to categorise" and marketing struggles because no genre audience claims them.
- **Experimental.** Negative-curvature regions where small perturbations diverge rapidly. Highest variance in outcome: breakthrough literary works emerge here, alongside incomprehensible failures.

This taxonomy is not metaphorical: each basin type corresponds to measurable curvature and gradient properties of $\mathcal{M}_N$ under the chosen k_{narr}. In editorial practice, basin classification provides an early-warning signal for manuscripts whose embedding sits in a repulsive zone.

8.8 Open problems

F. Zimmerman (2026e, Ch. 20) catalogues nine open problems in narrative mathematics; I restate the most important here as formal conjectures.

Conjecture 8.3 (Formal Vonnegut)**.** *The eigenvalue spectrum of the emotional-arc kernel on a sufficiently large fiction corpus exhibits a sharp drop after some index $K \in [6, 20]$. Equivalently, fiction admits a low-rank emotional-arc subspace, formalising Vonnegut (1981)'s informal claim about archetypal shapes.*

Reagan et al. (2016) produced experimental evidence consistent with $K = 6$ on a corpus of 1,327 Project Gutenberg novels using sentiment SVD; the conjecture predicts that more careful spectral analysis with k_{GA}-induced kernels will recover a similar plateau on much larger corpora.

Conjecture 8.4 (Adaptation Fidelity Bound)**.** *For any RKHS rank-K approximation $k_{\text{narr}}^{(K)}$ of the full narrative kernel, the maximum Wasserstein-fidelity adaptation $\widetilde{N}$ of source N satisfies*

$$W_2(N, \widetilde{N})^2 \;\geq\; \sum_{k>K} \lambda_k \, e_k(N)^2.$$

Discarded principal-component energy is a lower bound on adaptation distance.

Conjecture 8.5 (Kernel Composition)**.** *For non-trivial narrative subspaces V_1, V_2 that are not orthogonal, the projection-product kernel $k_1 \cdot k_2$ has spectrum strictly contained in $\sigma(k_1) \cap \sigma(k_2)$; i.e., products of overlapping kernels lose, rather than gain, eigenmodes.*

Conjecture 8.6 (Tversky Challenge)**.** *There exists a context-dependent kernel $k_\theta(\cdot, \cdot; C) : \mathcal{X} \times \mathcal{X} \times \mathcal{C} \to \mathbb{R}$ that is PSD for each fixed C and reproduces the asymmetry pattern in human similarity judgements $s(x, y; C) \neq s(y, x; C)$ (Tversky 1977) via post-projection of the symmetric kernel onto C-dependent subspaces.*

These conjectures are tractable: each is testable on existing corpora using off-the-shelf eigendecomposition or crowdsourced similarity judgements, and a positive resolution would strengthen the framework with quantitative guarantees that practical publishing pipelines can rely on.

9 Related Work

Distant reading and computational narratology. The lineage from Moretti (2005) through Jockers (2013) and Underwood (2019) is the immediate intellectual ancestor of this work. These

authors operate at the level of word frequencies, topic distributions, or sentiment trajectories. My framework lifts the analysis to the level of dense semantic embeddings while retaining the macroanalytic stance. Reagan et al. (2016) identified six emotional arcs in 1,327 Project Gutenberg novels via sentiment-curve SVD; I treat the emotional arc as one of many trajectories that can be GA-kernelled inside a richer narrative manifold.

Sentence embeddings. The tractability of the framework hinges on the availability of high-quality sentence encoders. Vaswani et al. (2017) introduced the Transformer; Devlin et al. (2019) the masked-language-model pretraining objective; Reimers and Gurevych (2019) fine-tuned Siamese/triplet networks on natural-language inference to produce embeddings suitable for cosine similarity. Current best-in-class encoders are tracked by the MTEB benchmark (Muennighoff et al. 2023).

Kernel methods for text. Lodhi et al. (2002) introduced string kernels for text classification; Cuturi (2011) introduced the Global Alignment Kernel that I adopt for arc and tension trajectories; Shervashidze et al. (2011) introduced the Weisfeiler–Lehman graph kernel that I adopt for escalation graphs; Kriege et al. (2020) surveys graph kernels more broadly.

Optimal transport for narrative. Villani (2009), Cuturi (2013), and Peyré and Cuturi (2019) provide the optimal transport machinery used in Section 7.5. I am aware of no prior work that applies optimal-transport *plans* as adaptation blueprints.

Information-theoretic novelty. The novelty-trajectory work in F. Zimmerman (2026d), F. Zimmerman (2026c), and W. F. Zimmerman (2026) operationalises Schmidhuber's compression-progress theory of interestingness (Schmidhuber 2009; Schmidhuber 2010) at the embedding level, and forms the empirical scaffolding underneath several findings in this paper. I summarise each paper in turn.

F. Zimmerman (2026d) introduced the running-centroid novelty measure used in Section 6.6 and applied it to a combined PG-19 / Books3 corpus of 81,526 full-length books. The principal findings were: (i) mean paragraph-level novelty roughly 10% higher in modern books (0.503 vs. 0.459), (ii) circuitousness nearly doubled in the modern corpus, (iii) convergent narrative shapes 2.3× more common in pre-1920 literature, and (iv) novelty essentially orthogonal to reader quality ratings ($r = -0.002$), implying that Schmidhuber-style interestingness is structurally independent of perceived merit. Clustering paragraph-level trajectories via PAA-16 representations recovered eight narrative-shape archetypes whose distribution shifts substantially between eras.

F. Zimmerman (2026a) described the toolkit underlying these analyses in implementation detail—unified SQL views, checkpoint/resume, `float16` storage with $r > 0.9999$ correlation against `float32`, and Streamlit deployment on a single GCP virtual machine. Five components are exposed: a Semantic Novelty Hub for PG-19, a Novelty Explorer for cross-corpus comparison, a PG-19 BISAC Browser implementing dual keyword and RKHS-semantic classification, a Thematic Anthology Engine that retrieves paragraphs across 28K+ books by query embedding, and a Republication Scorer that finds public-domain works whose novelty profiles match modern bestsellers.

F. Zimmerman (2026c) extended the framework with Symbolic Aggregate approXimation (Lin, Keogh, Lonardi, et al. 2003; Lin, Keogh, Wei, et al. 2007; Keogh et al. 2005). Each book's novelty curve was discretised into a 16-character SAX-5 string; the analysis identified the most common motifs (notably `cccc`: four consecutive segments of medium novelty, 11.8–12.3% of all 4-gram occurrences across both corpora), genre-specific fingerprints, and the dramatic free-verse vs. formal-verse circuitousness gap reported in Section 6.7.

W. F. Zimmerman (2026) scaled the measure to the IB1 Internet Archive corpus (452,796 books, 1500s–1940), an order of magnitude larger than any previous embedding-based trajectory analysis. The principal counterintuitive finding is that institutional texts (government reports, legislative proceedings, legal treatises) are *more* novel on average than literary texts of the same era, with Cohen's $d = 0.63$ and $p \approx 0$. Pivotal-year analysis with sufficient statistical power to detect $\Delta = 0.003$ identified the Congress of Vienna (1815) as the strongest pivotal effect on novelty ($\Delta = +0.023$, $d = 0.34$, $p = 5.5 \times 10^{-58}$), with the end of the US Civil War producing a strong nation-specific signal ($\Delta_{\text{US}} = +0.017$, $p = 8.1 \times 10^{-9}$). Genre analysis across 15 categories revealed a novelty hierarchy spanning $d = 1.24$ from law (lowest) to engineering (highest).

Doctrine morphing. F. Zimmerman (2026b) introduced ten morphological operators on a 105-doctrine RKHS and validated 16 generated concepts. The operators of Section 4.2.1 are direct restatements; the present paper additionally proves the algebraic properties (Theorems 4.2–4.4) that make the operators behave well under composition.

Tversky asymmetry. A standing tension in the framework is that human similarity judgements are asymmetric (Tversky 1977), while PSD kernels are symmetric by definition. I address this in Section 12.

Macroanalysis and digital humanities tradition. The macroanalytic turn in literary studies (Moretti 2005; Jockers 2013; Underwood 2019) provides the methodological license for the present paper. Moretti (2005) established that publication metadata, genre frequencies, and network topologies reveal patterns invisible to close reading; Jockers (2013) demonstrated that topic models and sentiment trajectories applied to nineteenth-century fiction reveal systematic differences across genres and genders; Underwood (2019) extended this work with HathiTrust-scale analyses, including longitudinal tests of canonicity. Story Operators inherits the macroanalytic stance but lifts the analytical unit from words and topics to embedding-space points and geometric/operator-algebraic structures. The trade-off is well known: dense embeddings are less interpretable per dimension than topic mixtures, but support a richer downstream algebra.

Distant-reading toolkits. The toolkit of Section 5.4 is closest in spirit to Voyant Tools (Sinclair and Rockwell 2016), the HathiTrust Research Center, and BookNLP (Bamman et al. 2014). These provide word-level frequency counts, named-entity recognition, and basic NLP pipelines at scale, but operate exclusively at the surface level. F. Zimmerman (2026a) argues that no prior public toolkit combines (i) sentence-level dense embeddings, (ii) interactive web UI, (iii) corpus-scale (10^4+ books), and (iv) novelty-trajectory visualisation. The Story Operators toolkit fills this gap.

Information theory and narrative. Shannon (1948) established the mathematical foundations for quantifying information content in text. Entropy-rate constancy (Genzel and Charniak 2002) predicts that per-sentence surprisal remains roughly constant within a text; the running-centroid measure used here generalises this to the embedding-space and shows that paragraph-level novelty is bounded but not constant. Chambers and Jurafsky (2008) extracted unsupervised narrative event chains from text; their event sequences could be embedded as RKHS feature vectors and analysed with the kernels of Section 3.4.

Information geometry. Amari (2016)'s information-geometric perspective treats families of probability distributions as Riemannian manifolds. In the present setting, replacing pointwise

narrative embeddings with distributions over local features (paragraphs, scenes) and using the Fisher–Rao metric in place of the cosine kernel produces a narrative information geometry whose practical relevance is an open question: information-geometric metrics may be more sensitive to fine structural distinctions than $k_{\cos}$, at the cost of considerably greater computational complexity.

Diachronic embedding studies. Hamilton et al. (2016) demonstrated that word embeddings track semantic change over centuries, establishing the prerequisite for diachronic embedding-based studies of the kind reported in Section 6.6. Michel et al. (2011) introduced the Google N-gram corpus and the paradigm of culturomics; the Story Operators framework extends that paradigm from word frequencies to embedding-based trajectory descriptors. Bayesian character modelling (Bamman et al. 2014) is complementary to the character-network kernels of Section 3.2.

10 Cost, Latency, and Operating Profile

The deployed framework has a distinctive cost profile that distinguishes it from API-based pipelines.

One-time vs. marginal cost. The entire CodexSpace embedding takes 8–10 hours on a single laptop CPU; the resulting $\sim$ 768 MB of embeddings and kernel indices is then queried at $\sim$ 50 ms per nearest-neighbour and $\sim$ 10 ms per operator application, with no further API or network costs. Books3 added 5–7 days of GPU compute for 52,796 books; IB1 added several weeks of distributed GPU compute for 452,796 books. In all three cases, once embedding is complete, all downstream operations run locally.

Per-pipeline cost. RKHS-First publishing for a single book typically requires:

- One full corpus search to seed each chapter ($\sim$ 50 ms per query, $\sim$ 20 queries per book).
- Several iterative refinement loops, each invoking an LLM for inverse embedding ($\sim$ 1–5 s per LLM call, several hundred calls per book).
- Final structural verification: convex-hull volume, minimum-pairwise-distance, centrality variance ($\sim$ 1 s each).

The dominant cost is LLM invocation, which scales with book length and revision aggressiveness rather than with corpus size.

Storage envelope. `float16` embeddings for 452,796 books occupy approximately 20 GB of SSD; the corresponding metadata SQLite databases are $\sim$ 1.1 GB (Books3) and $\sim$ 711 MB (PG-19) per corpus; per-paragraph novelty scores add $\sim$ 100 MB per corpus. Total disk footprint for the full deployed toolkit is under 30 GB, well within the capacity of a single SSD. This is the key engineering finding underwriting the public deployment: the framework runs on a single `e2-standard-2` virtual machine because the storage requirements are small enough to fit there.

Latency budget. Steady-state user-facing latencies on the deployed toolkit:

Operation	Latency
Single-book lookup	< 100 ms
Novelty trajectory render	< 500 ms
Corpus-wide aggregation	< 3 s
Cross-corpus comparison	< 2 s
Paragraph-level retrieval	< 5 s

These latencies suffice for interactive editorial use without caching or pre-aggregation. The bottleneck for further scaling is not query speed but Gram-matrix size; sharded indices or randomised features would be required for $> 10^6$-book corpora.

11 Codextype Taxonomy

Production experience with the framework on twenty-nine RKHS Integrated Series volumes (F. Zimmerman 2026e, App. E) produced seven recurring book templates—"codextypes"—each tuned to a particular combination of source material and analytical goal. I document them here because they are the empirical interface between the mathematical apparatus and editorial practice.

Table 9: Seven codextypes that recur in RKHS-First publishing.

ID	Name	Use case
RKHS-01	Corpus Analysis	Analytic perspective on 10–100 documents.
RKHS-02	Senior Leadership Leave-Behind	Single-topic POV with RKHS-backed evidence.
RKHS-03	Atlas with Plates	Visual reference to a 100+-document corpus.
RKHS-04	Encyclopedia of Transforms	Inclusive scenario generation from a corpus.
RKHS-05	Core Scenarios Book	Apparatus for four main scenarios.
RKHS-06	Concept Frontier Buster	Extension of ideas to their frontiers.
RKHS-07	Annotated Classic	Public-domain classic with RKHS enhancement.

The codextype taxonomy is the empirical complement to the six graph objectives of Section 6.5: the objectives specify the desired structural shape, and the codextype specifies the editorial conventions (page count, illustration density, front- and back-matter expectations) that turn the structural shape into a marketable book. In production I observe that a given graph objective tends to map onto a small number of codextypes: Maximum Coverage maps to RKHS-01 and RKHS-03; Polarised maps to RKHS-04 and RKHS-05; Hierarchical maps to RKHS-02 and the *rebooted* variant of RKHS-07.

12 Discussion and Limitations

Embedding bias. All numerical results depend on a sentence-transformer encoder trained on general English (and, for the BGE variant, a multilingual extension). Strategic terminology, archaic prose, and poetry are under-represented in the training data. Numerical similarities are meaningful relative to one another within a fixed model, but cannot be interpreted as absolute measurements (F. Zimmerman 2026e, Ch. 15).

Manifold conjecture. Conjecture 8.1 is supported empirically but unproven. A rigorous test would require either a generative model that produces provably on-manifold samples, or direct

estimation of the manifold's intrinsic dimension via Hausdorff or persistent-homology techniques (Edelsbrunner and Harer 2010; Reininghaus et al. 2015).

Operator interpretability. The doctrine, fiction, and poetry operators have well-defined mathematical forms, but their *semantic* interpretability is mediated by an LLM that turns target embeddings into readable text (Section 6.5). Errors in this inverse embedding step can produce coherent text whose embedding fails to hit the target, or vice versa.

Sample size for RKHS-First. The improvements in Table 5 are based on 13 RKHS-First volumes against matched controls. The author was the common pipeline operator; expectation effects cannot be ruled out. Larger blinded studies, with multiple authors and external coders, are required.

Tversky asymmetry. Human similarity judgments are asymmetric and dependent on context (Tversky 1977): "North Korea is similar to China" is judged more readily than the reverse. PSD kernels cannot reproduce this asymmetry directly. Two partial remedies are: (i) replacing $k(x, y)$ with a contextual divergence $k_\theta(x, y; C)$ that depends on a context C, accepting some loss of PSD; (ii) modelling asymmetry post-hoc as a directional bias on top of a symmetric kernel. This is Open Problem 7 of F. Zimmerman (2026e, Ch. 20).

Computational scope. The deployed toolkit handles $\sim 5 \times 10^5$ books on a single virtual machine. Larger corpora (10^7 books) are likely feasible with sharded indices, but the Gram-matrix size scales as $O(n^2)$ and would require approximate nearest-neighbour structures or randomized kernel features. Random Fourier features (Schölkopf and Smola 2002) provide a principled $O(nD)$ approximation for shift-invariant kernels (RBF), and could in principle replace the dense Gram matrix in the spectral analyses of Section 6.12 at modest accuracy cost.

Causality and direction. The empirical results in Section 6 are *descriptive*, not causal. I do not claim that applying an operator *causes* any particular human reader response, only that the operator induces a well-defined transformation in embedding space. Bridging from the embedding-space transformation to a causally validated reader-response prediction is a substantial open problem.

Vendor and model lock-in. The framework depends on a specific embedding model (all-mpnet-base-v2 or BGE-large-en-v1.5). Were either model deprecated, all numerical results would shift even though the qualitative geometry would be similar. I mitigate this risk by storing both raw text and the model version with each embedding, so that re-embedding is always possible.

Public-domain bias. PG-19 over-represents male, English, white, Western voices; women's autobiography, women's political writing, and non-Western texts are under-represented in the pre-1919 corpus (F. Zimmerman 2026e, Ch. 6). Findings about "literary structure" that draw exclusively from PG-19 must be qualified accordingly. The Books3 and IB1 extensions ameliorate this somewhat but do not solve it.

Operator interpretability via inverse embedding. A persistent threat is that operator outputs in $\mathcal{H}_N$ may have no faithful textual realisation: the inverse embedding problem is ill-posed. In practice, the LLM-driven inverse step (Section 6.5) produces text whose embedding matches the target with median Euclidean error < 0.05 in the pilots reported here, but the variance is high and

a tail of cases exists in which fluent text is generated whose embedding diverges by > 0.20 from the target. I treat such cases as production failures and flag them for human revision.

Reproducibility burden. A practical concern: full reproduction of the empirical results in this paper requires roughly ~ 100 GB of intermediate storage, several days of single-GPU compute (for Books3-scale embedding), and familiarity with the `sentence-transformers`, `POT`, and `python-igraph` libraries. I have made every effort to keep the format open and the toolkit deployable on a single commodity instance, but the framework is not yet "one-click." This is a target for future infrastructural work.

13 Conclusion and Future Work

I have presented Story Operators as a coherent mathematical framework for narrative analysis and transformation built on RKHS theory. The framework comprises (i) fifteen positive semi-definite narrative kernels, (ii) thirty-four bounded normalising operators, (iii) a deployed empirical apparatus on three corpora totalling more than half a million books, and (iv) a series of cross-domain applications—doctrine morphing, story liberation, RKHS-first publishing, optimal-transport adaptation, and federation—that demonstrate practical utility. All components are open and reproducible: the embeddings, kernels, operators, RKHS file format, and analysis toolkit are deployed publicly.

The main scientific contribution is the demonstration that *transformation* as well as *measurement* can be made mathematically precise on text. Once the operator algebra exists, the editorial questions practitioners ask informally—"what would this look like as a thriller, set in space, retold for middle-graders?"—become quantitative, composable, and reproducible.

Future work falls into three categories.

Theoretical. The principal open problems are: proving Conjectures 8.1 (Narrative Manifold), 8.2 (Genre Speciation), 8.3 (Formal Vonnegut), 8.4 (Adaptation Fidelity Bound), 8.5 (Kernel Composition), and 8.6 (Tversky Challenge). Two additional research problems from F. Zimmerman (2026e, Ch. 20) that I did not foreground but consider important are: (i) the persistent homology of character networks—do Edelsbrunner and Harer (2010) and Reininghaus et al. (2015)-style topological features detect narrative structure invisible to first-order spectral analysis?—and (ii) a category-theoretic perspective on operators, in which doctrine, fiction, and poetry operators are morphisms in suitable functor categories with composition expressible as natural transformations.

Empirical. Three priorities: (a) scaling to multilingual and cross-modal corpora using multilingual sentence transformers and CLIP-style image encoders; (b) testing the manifold hypothesis with persistent-homology techniques on the IB1 corpus; (c) validating RKHS-First publishing in larger blinded studies with multiple authors and external coders. The first will reveal whether the clusters and motifs reported here are language-universal or English-specific; the second is the natural geometric test of Conjecture 8.1; the third addresses the expectation-effect concern flagged in Section 12.

Infrastructural. The federation protocol of Section 7.9 needs hardening: cryptographic identity for universes, conflict resolution for concurrent edits, and a versioning system that scales across thousands of contributors. The toolkit's web interface—currently optimised for individual exploration—should

be extended with team-level workspaces, audit logs, and access controls suitable for institutional deployment.

The broader argument is that AGI-era publishing requires a mathematical operating system for content. Story Operators is one candidate.

The publishing context. The framework was developed in the context of an active publishing business that deploys it daily. Twenty-nine volumes in the RKHS Integrated Series have been produced under the RKHS-First workflow described in Section 6.5, with seven recurring *codextypes* (corpus analysis, senior leadership leave-behind, atlas with plates, encyclopedia of transforms, core scenarios, concept frontier buster, annotated classic) emerging as practical templates (F. Zimmerman 2026e, App. E). The four-tier free/consumer/pro/enterprise monetisation model documented in F. Zimmerman (2026e, Ch. 30) provides the economic runway for the public infrastructure described here. Sustaining this kind of mixed academic–commercial deployment is itself a research question: how does one keep public-facing tools open while funding their continued development? The Story Operators ecosystem—open kernels, open file format, deployed toolkit, paid power-user tier—is one answer.

Beyond text. The kernel-and-operator architecture is content-agnostic. Replacing the sentence-transformer encoder φ with an image encoder (CLIP-style) yields an analogous CodexSpace for visual narrative; replacing it with an audio encoder yields one for music or podcasts. All kernels in Section 3 that depend on φ only through inner products carry over verbatim; only the graph-, arc-, and theme-level kernels need re-engineering for the new modality. The framework therefore offers a portable mathematics of narrative across text, image, audio, and—in principle—any medium with a learned dense embedding.

A Appendix A: Formal Definitions

A.1 Narrative kernel as a feature map composition

For any base feature map $\varphi : \mathcal{X} \to \mathcal{H}_N$ and any pre-processing $\psi : \mathcal{X}' \to \mathcal{X}$, the composite $k(\psi(N_1), \psi(N_2))$ is PSD by Proposition 2.2 (3). This is the formal justification for using all-mpnet-base-v2 or BGE-large-en-v1.5 as black-box pre-processing.

A.2 Narrative manifold (formal)

Let $\mathcal{M}_N \subset \mathcal{H}_N$ be the (conjectured) image of the set of coherent narratives. At each $N \in \mathcal{M}_N$, $T_N\mathcal{M}_N$ is a finite-dimensional subspace of $\mathcal{H}_N$ with the orthogonal decomposition stated in Conjecture 8.1. The genre foliation $\mathcal{M}_N = \bigcup_g \mathcal{M}_g$ has each leaf $\mathcal{M}_g$ a smooth submanifold; literary fiction is special in that its leaf is the entire $\mathcal{M}_N$.

A.3 Wasserstein distance (narrative)

For narratives N_1, N_2 with element distributions μ_1, μ_2 on $\mathcal{H}_N$,

$$W_2(N_1, N_2)^2 = \min_{\pi \in \Pi(\mu_1, \mu_2)} \int \|x - y\|^2 \, \mathrm{d}\pi(x, y),$$

where $\Pi(\mu_1, \mu_2)$ is the set of couplings. The optimal π is the *adaptation blueprint* of Section 7.5. Sinkhorn entropic regularization (Cuturi 2013) gives fast approximate transport plans.

B Appendix B: Operator Catalog

The thirty-four operators in three domains. Notation: f is a unit-norm RKHS embedding; $c_\bullet$ a normalised centroid; $\widehat{\cdot}$ denotes normalisation.

B.1 Doctrine operators (10)

1. Adversarial Inversion: $\mathsf{T}(f) = \widehat{-f}$.
2. Temporal Shift: $\mathsf{T}(f; \alpha, \text{era}) = \widehat{(1-\alpha)f + \alpha c_{\text{era}}}$.
3. Escalation Gradient: $\mathsf{T}(f; \lambda) = \widehat{f + \lambda v_{\text{esc}}}$.
4. Cultural Translation: $\mathsf{T}(f; s, t) = \widehat{f - c_s + c_t}$.
5. Domain Projection: $\mathsf{T}(f; \alpha, \text{dom}) = \widehat{(1-\alpha)f + \alpha c_{\text{dom}}}$.
6. Actor Transformation: $\mathsf{T}(f; \alpha, \text{type}) = \widehat{(1-\alpha)f + \alpha c_{\text{actor}}}$.
7. Synthesis (Blend): $\mathsf{T}(\{f_i, w_i\}) = \widehat{\sum_i w_i f_i}$.
8. Constraint Projection: $\mathsf{T}(f; C) = f - \widehat{\sum_{c \in C} \langle f,\, c \rangle\, c}$.
9. Intensification: $\mathsf{T}(f; \alpha) = c_{\text{base}} + \widehat{\alpha(f - c_{\text{base}})}$.
10. Negation: $\mathsf{T}(f) = \widehat{c_{\text{all}} - f}$.

B.2 Fiction operators (14)

11. Character Removal: $G_N = (V, E, w) \mapsto G'_N = (V \setminus \{c^*\}, E', w')$ with edges incident to c^* deleted.
12. Character Merge: replace $\{c_1, c_2\} \subset V$ with a single node c_{12} whose edge weights are the union $w'(c_{12}, x) = w(c_1, x) + w(c_2, x) - w(c_1, c_2)$.
13. Relationship Inversion: edge sentiments $s(c, c') \mapsto -s(c, c')$.
14. Arc Compression: choose n time points minimising the information loss $\text{KL}(p_{\text{full}} \,\|\, p_{\text{compressed}})$.
15. Arc Expansion: Gaussian-weighted interpolation between selected key points.
16. Arc Reversal: reflect the arc trajectory about the orthogonal complement of the moral-axis subspace.
17. Arc Branch: from a decision point t^*, generate an alternative continuation a'_t for $t > t^*$ via a learned branching distribution.
18. Genre Transform: Theorem 4.2.
19. Perspective Transform: recenter narrative voice on a new character c^* via the corresponding character-state sub-embedding.
20. Setting Transform: replace setting-specific embedding components with target-setting averages.
21. Tension Resolution: collapse a tension toward one pole.
22. Tension Escalation: amplify tension intensity by a scalar.
23. Tension Transfer: redistribute energy between tensions while preserving total magnitude.
24. Stakes Scaling: scale all stakes by a common factor.

B.3 Poetry operators (10)

25. Word Substitution: replace word w_i in line ℓ with target w_i', preserving form constraints.
26. Negation: semantically negate a line via lexical or embedding-space negation operator.
27. Form Transform: change poetic form (sonnet $\to$ haiku) by re-targeting the form-constraint projection $P_{S_{\text{form}}}$.
28. Tradition Projection: decompose $f = P_{\text{conv}} f + (I - P_{\text{conv}})f$.
29. Influence Measurement: $\mathsf{T}(f) = \{\langle f,\, c_i\rangle\}_{i \in \text{canon}}$.
30. Rhyme Tension Analysis: $\mathsf{T}(f) = k_{\text{phon}} \cdot k_{\text{sem}}$.
31. Metrical Deviation: $\mathsf{T}(\ell) = \|m(\ell) - m_0\|_2$.
32. Repetition Pattern Analysis: per-occurrence cosine similarity with first occurrence.
33. Form Constraint Projection: orthogonal projection onto the span of form exemplars.
34. Intertextual Allusion Detection: $\arg\max k_{\text{phon}-\text{sem}}$ against canonical line corpus.

B.4 Operator algebra cheat-sheet

The thirty-four operators decompose into five algebraic patterns:

- **Reflection:** $\mathsf{T}(f) = \widehat{-f}$ (Inversion, Negation).
- **Convex blend:** $\mathsf{T}(f; \alpha, c) = \widehat{(1-\alpha)f + \alpha c}$ (Temporal Shift, Domain Projection, Actor Transformation, Synthesis).
- **Translation:** $\mathsf{T}(f; b) = \widehat{f + b}$ (Cultural Translation, Escalation Gradient, Setting Transform).
- **Linear projection:** $\mathsf{T}(f; P) = Pf$ or $(I - P)f$ (Constraint Projection, Tradition Projection, Form Constraint Projection).
- **Spectral scaling:** $\mathsf{T}(f) = \widehat{Af}$ with $A = \sum \lambda_k e_k e_k^\top$ (Intensification, Tension Escalation, Stakes Scaling).

This taxonomy clarifies why the operators compose well: each pattern preserves the essential structure of S^{d-1}, and pairwise compositions remain expressible as either (2) or its projection variant.

C Appendix C: Proof Sketches

I sketch the validity of representative kernels.

Proposition C.1 (Scene co-occurrence is PSD)**.** *Let $\varphi_{\text{sco}}(N) \in \mathbb{R}^{|V_{\text{global}}|^2}$ be the vectorised scene co-occurrence matrix. Then $k_{\text{sco}}(N_1, N_2) = \langle \varphi_{\text{sco}}(N_1),\, \varphi_{\text{sco}}(N_2)\rangle$ is PSD.*

Proof sketch. Direct: k_{sco} is an inner product in a Euclidean space, hence PSD by definition of PSD. □

Proposition C.2 (Composite character kernel is PSD)**.** $k_{\text{char}} = \alpha_1 k_{\text{sco}} + \alpha_2 k_{\text{dlg}} + \alpha_3 k_{\text{nf}}$ *with $\alpha_i \geq 0$ is PSD.*

Proof sketch. Each component is PSD; non-negative linear combinations of PSD kernels are PSD by Proposition 2.2 (1). □

Proposition C.3 (Arc kernel via GAK is PSD)**.** k_{GA} *defined as in Section 3.3 with local kernel* κ *PSD is PSD.*

Proof sketch. Cuturi (2011) shows that the Global Alignment Kernel built from a PSD local similarity is PSD; I instantiate κ with the RBF kernel. □

Proposition C.4 (Full narrative kernel is PSD)**.** k_{narr} *as in (1) is PSD whenever each component kernel is PSD and the weights are non-negative.*

Proof sketch. Apply Proposition 2.2 (1). □

A subtle case: signed dialogue. Naively defining k_{dlg} with signed sentiment counts breaks PSD, because the resulting Gram matrix can have negative eigenvalues for adversarial input. The fix is to decompose $\sigma = \sigma^+ + \sigma^-$ and form $k_{\mathrm{dlg}} = k^+_{\mathrm{dlg}} + k^-_{\mathrm{dlg}}$, each PSD by sum-of-products construction.

Proposition C.5 (Theme-activation kernel is PSD)**.** $k_{\mathrm{thm}}(N_1, N_2) = \widehat{\theta(N_1)}^{\top} \widehat{\theta(N_2)}$ *is PSD.*

Proof sketch. This is a normalised inner product on $\mathbb{R}^T$. Normalisation preserves PSD by Proposition 2.2 (5). □

Proposition C.6 (Theme competition kernel is PSD)**.** $k_{\mathrm{thm-comp}}(N_1, N_2) = \exp(-\gamma \left\|\theta(N_1) - \theta(N_2)\right\|^2)$ *is PSD on* Δ^{T-1}*.*

Proof sketch. RBF on any subset of $\mathbb{R}^T$ is PSD by Schoenberg's theorem; the simplex is a subset of $\mathbb{R}^T$, and the restricted kernel is the Gram matrix of the restricted index set, hence PSD. □

Proposition C.7 (Escalation graph kernel is PSD)**.** *The Weisfeiler–Lehman graph kernel (Shervashidze et al. 2011)* $k^{\mathrm{WL}}_{\mathrm{esc}}(G_{N_1}, G_{N_2})$ *on labelled escalation graphs is PSD.*

Proof sketch. Shervashidze et al. (2011) construct k^{WL} as a sum of PSD subtree-pattern kernels at each WL iteration; the iterated relabelling produces a finite-dimensional explicit feature map. □

Proposition C.8 (Composite character kernel is bounded)**.** *With* k_1, k_2, k_3 *each bounded above by* 1 *and* $\alpha_1 + \alpha_2 + \alpha_3 = 1$*,* $k_{\mathrm{char}} \le 1$ *pointwise.*

Proof sketch. Convex combination of values in $[0, 1]$. □

Operator boundedness. For each normalising operator of form (2) I have $\left\|\mathsf{T}(f)\right\|_{\mathcal{H}_N} = 1$, hence T is non-expansive on S^{d-1}: $d_{\mathcal{H}_N}(\mathsf{T}(f), \mathsf{T}(f')) \le 2$. In addition, when A is the identity perturbed by a rank-one update (e.g. for $\mathsf{T}_{\mathrm{cult}}, \mathsf{T}_{\mathrm{era}}, \mathsf{T}_{\mathrm{esc}}$), T is Lipschitz with constant $1 + \|b\|$ in ambient $\mathcal{H}_N$ before normalisation. These bounds give the basic stability guarantees needed for editorial pipelines that compose many operators sequentially.

D Appendix D: Cluster Statistics for CodexSpace

I provide the full 25-cluster breakdown of CodexSpace (F. Zimmerman 2026e, Ch. 6) for reference. Clusters are ordered by descending size; sizes sum to 28,044 books (the corpus subset retained for clustering, somewhat smaller than the 28,602 used for similarity search).

Table 10: All twenty-five CodexSpace clusters under BGE-large-en-v1.5 embeddings.

ID	Name	Size	%
14	Victorian Popular Fiction & Serials	4,353	15.5
7	History, Biography & Travel	3,921	14.0
0	Adventure Fiction & Boys' Stories	3,567	12.7
23	Reference, Religion & Practical	3,473	12.4
10	Literary Fiction & Collected Tales	2,733	9.7
5	Poetry & Drama	2,160	7.7
19	Devotional & Inspirational	1,321	4.7
13	American Periodicals & Miscellany	1,216	4.3
2	English Poetry & Drama Collections	1,214	4.3
17	Reference Periodicals & Notes	1,041	3.7
6	Trade Periodicals	730	2.6
22	Continental Translations	612	2.2
9	American Gothic / Hawthorne School	465	1.7
16	Irish Penny Press	408	1.5
24	Theatre Reviews	357	1.3
21	Children's Picture Books	317	1.1
1	Genealogy and Local History	287	1.0
3	Children's Chapter Books	241	0.9
8	Children's Verse	198	0.7
18	American Civil War	155	0.6
20	Cookery and Domestic	122	0.4
15	Government Documents	103	0.4
12	*Punch* Magazine Issues	71	0.3
4	Religious Pamphlets / African Amer.	49	0.2
11	George Borrow Translations	30	0.1
	Total	**28,044**	**100.0**

The size distribution is heavily skewed: top three clusters cover 42.2%, top five cover 64.3%, top ten cover 88.3%. The remaining fifteen clusters share 11.7% of the corpus but provide the most precise authorial and publication-project signatures (George Borrow translations, *Punch* issues, religious pamphlets, Irish penny press, government documents).

E Appendix E: Reproducibility

Models. sentence-transformers/all-mpnet-base-v2 (768-dim) and BAAI/bge-large-en-v1.5 (1024-dim). Both are publicly available on Hugging Face.

Corpora. PG-19 (Rae et al. 2020); Books3 (no longer redistributed; I retain only aggregate statistics) (Gao et al. 2021); IB1 (Internet Archive, batch 1) (W. F. Zimmerman 2026).

Software. `sentence-transformers` (v2.x+), `numpy`, `scikit-learn`, `pandas`, `POT` (optimal transport), `python-igraph` (Weisfeiler–Lehman), custom `RKHSPipeline` class (F. Zimmerman 2026e, Ch. 22).

Storage. SQLite (book metadata, per-book metrics, per-paragraph novelty), NumPy memory-mapped `float16` arrays for embeddings. Pearson $r > 0.9999$ between `float32` and `float16` cosine similarities.

Deployment. Streamlit on GCP `e2-standard-2` (2 vCPU, 8 GB RAM, SSD persistent disk), Apache 2 reverse proxy. Public URL `https://bigfivekiller.online`.

Minimal reproducible example. A representative end-to-end pipeline, omitting error handling:

```
from sentence_transformers import SentenceTransformer
import numpy as np

model = SentenceTransformer("all-mpnet-base-v2")
texts = ["...book␣A...", "...book␣B...", "...book␣C..."]
embeddings = model.encode(texts, normalize_embeddings=True)

# Cosine kernel = inner product on unit vectors.
K = embeddings @ embeddings.T

# Cultural Translation operator (T_cult).
def T_cult(f, c_source, c_target):
    g = f - c_source + c_target
    return g / np.linalg.norm(g)

# Genre Transform via projection (T_genre).
def T_genre(f, P_source, P_target, c_target):
    g = (np.eye(len(f)) - P_source) @ f + P_target @ f + c_target
    return g / np.linalg.norm(g)
```

A more complete pipeline that includes paragraph segmentation, running-centroid novelty computation, SAX symbolisation, and the five toolkit components is shipped with the public toolkit; the scaffold above suffices to replicate any single-book operator application.

Hardware envelope. Computing the full 28,602 × 28,602 Gram matrix for CodexSpace requires ~ 6.5 GB of `float64` or ~ 1.6 GB of `float16` memory. Embedding the entire PG-19 corpus from scratch on a 2024-vintage M-series Apple laptop takes $\sim$ 8–10 hours; on a single A100 GPU, ~ 30 minutes. Books3 (52,796 books) embedding takes 5–7 days on single GPU. IB1 (452,796 books) embedding, the largest in my experience, took several weeks of distributed GPU compute and required checkpoint/resume to survive interruptions.

F Postscript: An Operating System for Content

I close with a non-mathematical observation that motivates the mathematical content of the paper. The advent of large language models has changed the marginal cost of text generation from non-zero to approximately zero. In every previous era of publishing, scarcity of text constrained editorial workflows: acquisition was selective because a publisher could not commission infinite manuscripts; revision was constrained because a reviser's time is finite; adaptation was rare because each adaptation required months of expert labour. These constraints are gone.

What replaces them is a constraint of *structure*: in a world of infinite candidate text, the editorial question becomes *which* text to generate, in which configuration, to which end. The mathematical

operating system this paper proposes is one attempt to answer that question quantitatively. The kernels measure which texts are similar; the operators specify which transformations are coherent; the manifold and spectral analysis reveal which regions of the space are dense, sparse, or curved; and the applications—doctrine morphing, story liberation, RKHS-first publishing, optimal-transport adaptation—demonstrate that the operating system can in fact run real publishing pipelines.

The framework is unfinished. Several conjectures (Section 6 and Section 8) remain open; the operator catalogue (Appendix B) almost certainly excludes operators that practice will eventually demand; the Tversky tension (Section 12) is unresolved. But the framework exists, the empirical apparatus is deployed and reproducible, and the publishing infrastructure on which it runs is open. I invite researchers, publishers, and analysts to extend it—to add new kernels, propose new operators, find new sparse regions, refute the conjectures, and use the toolkit on their own corpora. Story Operators is not a finished theorem but a working invitation to a quantitative computational narratology.

Acknowledgements

This paper distils the second edition of *Story Operators* (F. Zimmerman 2026e) for an academic readership, drawing on empirical results first reported in F. Zimmerman (2026b), F. Zimmerman (2026d), F. Zimmerman (2026a), F. Zimmerman (2026c), and W. F. Zimmerman (2026). The Story Operators framework was developed at Nimble Books LLC and deployed on `https://bigfivekiller.online`. Deployment infrastructure runs on Google Cloud Platform. The author thanks the maintainers of `sentence-transformers`, `POT`, `python-igraph`, and `scikit-learn` for the open-source libraries on which this work depends. All embedding files, kernel implementations, operator code, and the `.rkhs.json` format specification are publicly available through the toolkit URL.

References

Amari, Shun-ichi (2016). *Information Geometry and Its Applications*. Springer.

Aronszajn, N. (1950). "Theory of reproducing kernels". In: *Transactions of the American Mathematical Society* 68.3, pp. 337–404.

Bamman, David, Ted Underwood, and Noah A. Smith (2014). "A Bayesian mixed effects model of literary character". In: *Proceedings of the 52nd Annual Meeting of the Association for Computational Linguistics (ACL)*.

Berlinet, Alain and Christine Thomas-Agnan (2004). *Reproducing Kernel Hilbert Spaces in Probability and Statistics*. New York: Springer.

Chambers, Nathanael and Dan Jurafsky (2008). "Unsupervised learning of narrative event chains". In: *Proceedings of the 46th Annual Meeting of the Association for Computational Linguistics (ACL)*.

Clausewitz, Carl von (1832). *On War*. Translated by M. Howard and P. Paret, Princeton University Press, 1976.

Cuturi, Marco (2011). "Fast global alignment kernels". In: *Proceedings of the 28th International Conference on Machine Learning (ICML)*.

— (2013). "Sinkhorn distances: Lightspeed computation of optimal transport". In: *Advances in Neural Information Processing Systems (NeurIPS)*.

Devlin, Jacob, Ming-Wei Chang, Kenton Lee, and Kristina Toutanova (2019). "BERT: Pre-training of deep bidirectional transformers for language understanding". In: *Proceedings of NAACL-HLT*.

Edelsbrunner, Herbert and John Harer (2010). *Computational Topology: An Introduction*. American Mathematical Society.

Gao, Leo, Stella Biderman, Sid Black, Laurence Golding, Travis Hoppe, Charles Foster, Jason Phang, Horace He, Anish Thite, Noa Nabeshima, Shawn Presser, and Connor Leahy (2021). *The Pile: An 800GB dataset of diverse text for language modeling*. arXiv: 2101.00027.

Genzel, Dmitriy and Eugene Charniak (2002). "Entropy rate constancy in text". In: *Proceedings of the 40th Annual Meeting of the Association for Computational Linguistics (ACL)*.

Hamilton, William L., Jure Leskovec, and Dan Jurafsky (2016). "Diachronic word embeddings reveal statistical laws of semantic change". In: *Proceedings of the 54th Annual Meeting of the Association for Computational Linguistics (ACL)*.

Jockers, Matthew L. (2013). *Macroanalysis: Digital Methods and Literary History*. University of Illinois Press.

Keogh, Eamonn, Jessica Lin, and Ada Fu (2005). "HOT SAX: Efficiently finding the most unusual time series subsequence". In: *Proceedings of the IEEE International Conference on Data Mining (ICDM)*.

Kriege, Nils M., Fredrik D. Johansson, and Christopher Morris (2020). "A survey on graph kernels". In: *Applied Network Science* 5, p. 6.

Labatut, Vincent and Xavier Bost (2019). "Extraction and analysis of fictional character networks: A survey". In: *ACM Computing Surveys* 52.5.

Lin, Jessica, Eamonn Keogh, Stefano Lonardi, and Bill Chiu (2003). "A symbolic representation of time series, with implications for streaming algorithms". In: *Proceedings of the 8th ACM SIGMOD Workshop on Research Issues in Data Mining and Knowledge Discovery*.

Lin, Jessica, Eamonn Keogh, Li Wei, and Stefano Lonardi (2007). "Experiencing SAX: A novel symbolic representation of time series". In: *Data Mining and Knowledge Discovery* 15.2, pp. 107–144.

Lodhi, Huma, Craig Saunders, John Shawe-Taylor, Nello Cristianini, and Chris Watkins (2002). "Text classification using string kernels". In: *Journal of Machine Learning Research* 2, pp. 419–444.

Mackinder, Halford J. (1904). "The geographical pivot of history". In: *The Geographical Journal* 23.4, pp. 421–437.

Michel, Jean-Baptiste, Yuan Kui Shen, Aviva Presser Aiden, Adrian Veres, Matthew K. Gray, Google Books Team, Joseph P. Pickett, Dale Hoiberg, Dan Clancy, Peter Norvig, Jon Orwant, Steven Pinker, Martin A. Nowak, and Erez Lieberman Aiden (2011). "Quantitative analysis of culture using millions of digitized books". In: *Science* 331.6014, pp. 176–182.

Moretti, Franco (2005). *Graphs, Maps, Trees: Abstract Models for a Literary History*. Verso.

Muennighoff, Niklas, Nouamane Tazi, Loïc Magne, and Nils Reimers (2023). "MTEB: Massive text embedding benchmark". In: *arXiv preprint arXiv:2210.07316*.

Peyré, Gabriel and Marco Cuturi (2019). "Computational optimal transport". In: *Foundations and Trends in Machine Learning* 11.5–6, pp. 355–607.

Rae, Jack W., Anna Potapenko, Siddhant M. Jayakumar, and Timothy P. Lillicrap (2020). "Compressive Transformers for long-range sequence modelling". In: *International Conference on Learning Representations (ICLR)*. Introduces the PG-19 dataset.

Reagan, Andrew J., Lewis Mitchell, Dilan Kiley, Christopher M. Danforth, and Peter Sheridan Dodds (2016). "The emotional arcs of stories are dominated by six basic shapes". In: *EPJ Data Science* 5.1, p. 31.

Reimers, Nils and Iryna Gurevych (2019). "Sentence-BERT: Sentence embeddings using Siamese BERT-networks". In: *Proceedings of the 2019 Conference on Empirical Methods in Natural Language Processing (EMNLP)*.

Reininghaus, Jan, Stefan Huber, Ulrich Bauer, and Roland Kwitt (2015). "A stable multi-scale kernel for topological machine learning". In: *IEEE Conference on Computer Vision and Pattern Recognition (CVPR)*.

Schmidhuber, Jürgen (2009). "Driven by compression progress: A simple principle explains essential aspects of subjective beauty, novelty, surprise, interestingness, attention, curiosity, creativity, art, science, music, jokes". In: *Anticipatory Behavior in Adaptive Learning Systems*. Springer.

— (2010). "Formal theory of creativity, fun, and intrinsic motivation". In: *IEEE Transactions on Autonomous Mental Development* 2.3, pp. 230–247.

Schölkopf, Bernhard and Alexander J. Smola (2002). *Learning with Kernels: Support Vector Machines, Regularization, Optimization, and Beyond*. Cambridge, MA: MIT Press.

Shannon, Claude E. (1948). "A mathematical theory of communication". In: *The Bell System Technical Journal* 27, pp. 379–423, 623–656.

Shervashidze, Nino, Pascal Schweitzer, Erik Jan van Leeuwen, Kurt Mehlhorn, and Karsten M. Borgwardt (2011). "Weisfeiler-Lehman graph kernels". In: *Journal of Machine Learning Research* 12, pp. 2539–2561.

Sinclair, Stefan and Geoffrey Rockwell (2016). "Voyant Tools". In: *Web tool, voyant-tools.org*.

Steinwart, Ingo and Andreas Christmann (2008). *Support Vector Machines*. New York: Springer.

Sun Tzu (500). *The Art of War*. Approx. 500 BCE. Translated by S. B. Griffith, Oxford University Press, 1963.

Tversky, Amos (1977). "Features of similarity". In: *Psychological Review* 84.4, pp. 327–352.

Underwood, Ted (2019). *Distant Horizons: Digital Evidence and Literary Change*. University of Chicago Press.

Vaswani, Ashish, Noam Shazeer, Niki Parmar, Jakob Uszkoreit, Llion Jones, Aidan N. Gomez, Łukasz Kaiser, and Illia Polosukhin (2017). "Attention is all you need". In: *Advances in Neural Information Processing Systems (NeurIPS)*.

Villani, Cédric (2009). *Optimal Transport: Old and New*. Springer.

Vonnegut, Kurt (1981). *Palm Sunday: An Autobiographical Collage*. Delacorte Press.

Zimmerman, Fred (2026a). "A web-accessible toolkit for large-scale semantic novelty analysis of literary corpora". arXiv-style preprint, Nimble Books LLC / BigFiveKiller.online.

— (2026b). "Morphological operators for strategic doctrine generation: A reproducing kernel Hilbert space framework". arXiv-style preprint, Nimble Books LLC; supersedes earlier "Thorn AI" draft (December 2025).

— (2026c). "SAX motif discovery in narrative novelty curves: Literary DNA across two centuries". arXiv-style preprint, Nimble Books LLC / BigFiveKiller.online.

— (2026d). "Semantic novelty trajectories in 80,000 books: A cross-corpus embedding analysis". arXiv-style preprint, Nimble Books LLC / BigFiveKiller.online.

— (2026e). *Story Operators: A Mathematical Framework for Narrative Discovery and Transformation*. Second. ISBN 978-1-60888-535-0; v2.0.1, April 2026. Ann Arbor, MI: Story Operators New Media.

Zimmerman, W. Frederick (2026). "Semantic novelty at institutional scale: Embedding-based trajectory analysis of 452,000 books from the Internet Archive". arXiv-style preprint, Nimble Books LLC.